Ecological Controls on N_2O Emission in Surface Litter and Near-surface Soil of a Managed Grassland: Modelling and Measurements

Grant, R.F.[1], Neftel, A.[2] and Calanca, P.[2]

[1] *Department of Renewable Resources, University of Alberta, Edmonton, AB, Canada T6G 2E3*

[2] *Agroscope Institute for Sustainability Sciences ISS, Reckenholzstrasse 191 , P.O. Box CH – 8046 Zürich, Switzerland*

ABSTRACT

Large variability in N_2O emissions from managed grasslands may occur because most emissions originate in surface litter or near-surface soil where variability in soil water content (θ) and temperature (T_s) is greatest. To determine whether temporal variability in θ and T_s of surface litter and near-surface soil could explain that in N_2O emissions, a simulation experiment was conducted with *ecosys*, a comprehensive mathematical model of terrestrial ecosystems in which processes governing N_2O emissions were represented at high temporal and spatial resolution. Model performance was verified by comparing N_2O emissions, CO_2 and energy exchange, and θ and T_s modelled by *ecosys* with those measured by automated chambers, eddy covariance (EC) and soil sensors at an hourly time-scale during several emission events from 2004 to 2009 in an intensively managed pasture at Oensingen, Switzerland. Both modelled and measured events were induced by precipitation following harvesting and subsequent fertilizing or manuring. These events were brief (2 – 5 days) with maximum N_2O effluxes that varied from < 1 mg N m^{-2} h^{-1} in early spring and autumn to > 3 mg N m^{-2} h^{-1} in summer. Only very small emissions were modelled or measured outside these events. In the model, emissions were generated almost entirely in surface litter or near-surface (0 – 2 cm) soil, at rates driven by N availability with fertilization vs. N uptake with grassland regrowth, and by O_2 supply controlled by litter and soil wetting relative to O_2 demand from microbial respiration. In the model, NO_x availability relative to O_2 limitation governed both the reduction of more oxidized electron acceptors to N_2O and the reduction of N_2O to N_2, so that the magnitude of N_2O emissions was not simply related to surface and

near-surface θ and T_s. Modelled N_2O emissions were found to be sensitive to defoliation intensity and timing which controlled plant N uptake and soil θ and T_s prior to and during emission events. Reducing LAI remaining after defoliation to one-half that under current practice and delaying harvesting by 5 days raised modelled N_2O emissions by as much as 80% during subsequent events and by an average of 43% annually. Modelled N_2O emissions were also found to be sensitive to surface soil properties. Increasing near-surface bulk density by 10% raised N_2O emissions by as much as 100% during emission events and by an average of 23% annually. Relatively small spatial variation in management practices and soil surface properties could therefore cause the large spatial variation in N_2O emissions commonly found in field studies. The global warming potential from annual N_2O emissions in this intensively managed grassland largely offset those from net C uptake in both modelled and field experiments. However model results indicated that this offset could be adversely affected by suboptimal land management and soil properties.

INTRODUCTION

The contribution of managed grasslands to reducing atmospheric greenhouse gas (GHG) concentrations through net uptake of CO_2 (Ammann et al., 2005) may be at least partially offset by net emissions of N_2O (Conant et al., 2005, Fléchard et al., 2005). These emissions may be substantial, with N_2O emission factors of as large as 3% measured in intensively managed grasslands with fertilizer rates of 25 - 30 g N m^{-2} y^{-1} (Imer et al., 2013; Rafique et al., 2011) These emissions are highly variable temporally and spatially because they are determined by complex interactions among short-term weather events (warming, precipitation), land management practices (N amendments, defoliation), and soil properties (e.g. bulk density, water retention). The N_2O driving these emissions in managed grasslands is thought to be generated within the upper 2 cm of the soil profile (van der Weerden et al., 2013) and in surface litter left by grazing or harvesting (Pal et al., 2013) so that diurnal heating and precipitation events that cause rapid warming and wetting of the litter and soil surface may cause large but brief emission events. These events are thought to be driven by increased demand for electron acceptors by nitrification and denitrification, and reduced supply of O_2 by which these demands are preferentially met, and therefore increased demand for alternative acceptors NO_3^-, NO_2^- and N_2O by autotrophic nitrifiers and heterotrophic denitrifiers.

The magnitude of N_2O emission events in managed grasslands generally increases with the amount of N added as urine, manure or fertilizer, and with the intensity of defoliation by grazing or cutting (Ruzjerez et al. 1994). Thus Imer et al. (2013) found a negative correlation between LAI and N_2O emissions at intensively managed grasslands in Switzerland. The increase in emissions with defoliation has been attributed to increased urine and manure deposition and soil compaction with defoliation by grazing, and to slower uptake of N and water by slower-growing plants with defoliation by harvesting (Jackson et al., 2015). Both N additions and defoliation are thought to raise these emissions by increasing the supply of NH_4^+ and NO_3^- to autotrophic nitrifiers and heterotrophic denitrifiers. This increase raises the demand for alternative e^- acceptors by these microbial populations if the supply of O_2, the preferred e- acceptor, fails to meet demand, as may occur when soil water content (θ) after defoliation rises with precipitation or reduced transpiration. This supply is governed by physical and hydrological properties (porosity, water retention) of the near-surface soil. Consequently land use practices and soil properties must be considered when estimating N_2O emissions from managed grasslands.

Recognition of the effects of precipitation events, N amendments and soil properties on N_2O emissions has led to empirical models in which annual emission inventories are calculated directly from annual precipitation and N inputs (Lu et al., 2006), or monthly emission events are calculated from monthly precipitation, air temperature T_a, and θ (Fléchard et al., 2007). However the soil depth at which most emitted N_2O is generated (0 – 2 cm) is much shallower than that at which θ used in these models is measured (5 – 10 cm) (Fléchard et al., 2007), and the soil temperature T_s at this depth may differ from T_a This is particularly so for grasslands in which N additions are necessarily left on the soil surface without incorporation. Thus large N_2O emissions may be caused by surface wetting from precipitation on dry soils following fertilizer application, so that deeper θ is sometimes found to be of little explanatory value in empirical models (Fléchard et al., 2007). Furthermore the response of denitrification to θ has been found in experimental studies to rise sharply with T_s, likely through the combined effects of T_s on increasing demand and reducing supply of O_2 at microbial microsites (Craswell, 1978). The interaction between T_s and θ on N_2O emissions is clearly apparent in the meta-analysis of N_2O emissions from European grasslands by Fléchard et al. (2007). This interaction has been represented in empirical models by fitting interdependent threshold values of T_s and θ above which emissions have been measured in field experiments (Smith and Massheder, 2014). However a more robust simulation of this interaction on

N_2O emissions should be built from basic biological and physical processes that are independent of site-specific measurements.

Process models used to simulate N_2O emissions from managed grasslands must therefore explicitly represent the effects of short-term weather events on near-surface T_s and θ, as well as the effects of N additions and defoliation on near-surface NH_4^+ and NO_3^-. These models must also explicitly represent the effects of mineral N, T_s and θ, and of soil physical and hydrological properties, on the demand for vs. supply of O_2 and alternative e^- acceptors NO_3^-, NO_2^- and N_2O, and on the oxidation-reduction reactions by which these e^- acceptors are reduced. However earlier process models have usually simulated N_2O emissions as T_s -dependent functions of nitrification and denitrification rates, modified by texture-dependent functions of water-filled pore space (WFPS) (e.g. Li et al., 2005). In some models additional empirical functions of T_s (Chatskikh et al., 2005), or of T_s and WFPS (Schmid et al., 2001), are used to calculate the fraction of nitrification that generates N_2O, and the fraction of heterotrophic respiration R_h that drives denitrification (Schmid et al., 2001), thereby avoiding the explicit simulation of O_2 and its control on N_2O emissions. A more detailed summary of functions of mineral N, T_s and WFPS currently used to model N_2O emissions is given in Fang et al. (2015). These functions have many model-dependent parameters and function independently of each other, so that key interactions among reduced C and N substrates, T_s and θ on N_2O production may not be simulated. In none of these approaches are the oxidation-reduction reactions by which N_2O is generated or consumed explicitly represented. Furthermore the effects of defoliation and surface litter on N_2O emissions have not been considered in earlier process models.

Process models used to simulate N_2O emissions must also accurately represent the key processes of C cycling that drive those of N cycling from which N_2O is generated and consumed. These include gross and net primary productivity (GPP and NPP) which drive mineral N uptake and assimilation with plant growth. GPP and consequent plant growth also drive autotrophic respiration (R_a), the below-ground component of which contributes to soil O_2 demand. NPP drives litterfall and root exudation, which in turn drive heterotrophic respiration (R_h) that also contributes to litter and soil O_2 demand, and thereby to demand for alternative e^- acceptors which drive N_2O generation. Heterotrophic respiration also drives key N transformations such as mineralization/immobilization, thereby controlling availability of these alternative e^- acceptors. Land use practices such as defoliation from grazing or harvesting, and

soil properties such as porosity and water retention, alter these key C cycling processes, and thereby N_2O emissions. Therefore these emissions are best simulated by comprehensive ecosystem models.

In the mathematical model *ecosys*, the effects of weather and N amendments on T_s, θ, and mineral N, and hence on the demand for vs. supply of O_2, NO_3^-, NO_2^- and N_2O, and thereby on N_2O emissions, are simulated by explicitly coupling the transport processes with the oxidation – reduction reactions by which these e^- acceptors are known to be generated, transported and consumed in soils (Grant and Pattey, 1999, 2003, 2008; Grant et al., 2006; Metivier et al., 2009). The development of model algorithms for these processes was guided by two key principles:

(1) all algorithms in the model must represent physical, biochemical and biological processes studied in basic research programs (e.g. convective-diffusive transport, oxidation-reduction reactions) so that these algorithms can be parameterized independently of the model

(2) this parameterization must be conducted at spatial and temporal scales smaller than those of prediction (in this case seasonal N_2O fluxes) so that site-specific effects on predicted values are not incorporated into the algorithms, limiting their robustness.

These principles are designed to avoid as much as possible the use of site- and model-specific algorithms that may lack application in sites and models other than those for which they were developed. Although models based on these principles appear complex, they can be better constrained than simpler models because they are parameterized from independent experiments. The resulting detail that application of these principles brings to the model enables better constrained tests of model output against more comprehensive and diverse site data than are possible with simpler models.

In an extension of earlier work with *ecosys*, we propose that temporal and spatial variation in N_2O emissions from an intensively managed grassland can be largely explained from the modelled effects of N amendments (fertilizer, manure), plant management (e.g. harvest intensity and timing), soil properties (e.g. bulk density) and weather (T_s, precipitation events) on the demand for vs. supply of O_2, NO_3^-, NO_2^- and N_2O in surface litter and near-surface soil (0 – 2 cm). Testing this explanation requires frequent measurements to characterize the large temporal variation in N_2O emissions found in managed ecosystems. Such measurements were recorded from 2004 to 2009 using automated chambers in

intensively managed grass-clover grassland at Oensingen, Switzerland, and used here to test our modelled explanation of these fluxes.

MODEL DEVELOPMENT

General Overview

The hypotheses for N_2O oxidation-reduction reactions and their coupling with gas transport in *ecosys* are represented in Fig. 1 and described further below with reference to equations and definitions listed in Appendices A, C, D, E, H of the Supplement (indicated by square brackets in the text below, e.g. [H1] refers to Eq. 1 in Appendix H), as well as in earlier papers (Grant and Pattey, 1999, 2003, 2008; Grant et al., 2006; Metivier et al., 2009). These hypotheses are part of a larger model of soil C, N and P transformations (Grant et al., 1993a,b), coupled to one of soil water, heat and solute transport in surface litter and soil layers, which are in turn components of the comprehensive ecosystem model *ecosys* (Grant, 2001).

Mineralization and Immobilization of Ammonium by All Microbial Populations

Heterotrophic microbial populations *m* (obligately aerobic bacteria, obligately aerobic fungi, facultatively anaerobic denitrifiers, anaerobic fermenters, acetotrophic methanogens, and obligately aerobic and anaerobic non-symbiotic diazotrophs) are associated with each organic substrate *i* (*i* = animal manure, coarse woody plant residue, fine non-woody plant residue, particulate organic matter, or humus). Autotrophic microbial populations *n* (aerobic NH_4^+ and NO_2^- oxidizers, hydrogenotrophic methanogens and methanotrophs) are associated with inorganic substrates. These populations grow with energy generated from coupled oxidation of reduced dissolved C (DOC) by heterotrophs, or of mineral N (NH_4^+ and NO_2^-) by nitrifiers, and reduction of e- acceptors O_2 and NO_x. These populations decay according to first-order rate constants with provision for internal recycling of limiting nutrients (N, P). During growth, each functional component *j* (*j* = nonstructural, labile, resistant) of these populations seeks to maintain a set C:N ratio by mineralizing NH_4^+ ([H1a]) from, or by immobilizing NH_4^+ ([H1b]) or NO_3^- ([H1c]) to, microbial nonstructural N. Nitrogen limitations during growth may cause C:N ratios to rise above set values, and greater recovery of microbial N from structural to nonstructural forms to

reduce N loss during decay, but at a cost to microbial function. These transformations control the exchange of N between organic and inorganic states, and hence affect the availability of alternative e^- acceptors for nitrification and denitrification.

Oxidation of DOC and Reduction of Oxygen by Heterotrophs

Constraints on heterotrophic oxidation of DOC imposed by O_2 uptake are solved in four steps:

1) DOC oxidation under non-limiting O_2 is calculated from active biomass, DOC concentration, and an Arrhenius function of T_s [H2],
2) O_2 reduction to H_2O under non-limiting O_2 (O_2 demand) is calculated from 1) using a set respiratory quotient [H3],
3) O_2 reduction to H_2O under ambient O_2 is calculated from radial O_2 diffusion through water films of thickness determined by soil water potential [H4a] coupled with active uptake at heterotroph surfaces driven by 2) [H4b]. O_2 diffusion and active uptake is calculated for each heterotrophic population associated with each organic substrate, allowing [H4] to calculate lower O_2 concentrations at microbial surfaces associated with more biologically active substrates (e.g. manure, litter). Localized zones of low O_2 concentration (hotspots) are thereby simulated when O_2 uptake by any aerobic population is constrained by O_2 diffusion to that population. O_2 uptake by each heterotrophic population also accounts for competition for O_2 uptake with other heterotrophs, nitrifiers, roots and mycorrhizae, calculated from its O_2 demand relative to those of other aerobic populations.
4) DOC oxidation to CO_2 under ambient O_2 is calculated from 2) and 3) [H5]. The energy yield of DOC oxidation drives the uptake of additional DOC for construction of microbial biomass $M_{i,h}$ according to construction energy costs of each heterotrophic population [A21]. Energy costs of denitrifiers are larger than those of obligately aerobic heterotrophs, placing denitrifiers at a competitive disadvantage for growth and hence DOC oxidation that declines with greater use of e^- acceptors other than O_2.

Oxidation of DOC and Reduction of Nitrate, Nitrite and Nitrous Oxide by Denitrifiers

Constraints imposed by NO_3^- availability on DOC oxidation by denitrifiers are solved in five steps:

1) NO_3^- reduction to NO_2^- under non-limiting NO_3^- is calculated from electrons demanded by DOC oxidation to CO_2 but met by O_2 reduction to H_2O because of diffusion limitations to O_2 supply, and hence transferred to NO_3^- [H6],

2) NO_3^- reduction to NO_2^- under ambient NO_3^- is calculated from 1), accounting for relative concentrations and affinities of NO_3^- and NO_2^- [H7],

3) NO_2^- reduction to N_2O under ambient NO_2^- is calculated from demand for electrons not met by NO_3^- reduction in 2), accounting for relative concentrations and affinities of NO_2^- and N_2O [H8],

4) N_2O reduction to N_2 under ambient N_2O is calculated from demand for electrons not met by NO_2^- reduction in 3) [H9],

5) additional DOC oxidation to CO_2 enabled by NO_x reduction in 2), 3) and 4) is added to that enabled by O_2 reduction from [H5], the energy yield of which drives additional DOC uptake for construction of $M_{i,n}$. This additional uptake offsets the disadvantage incurred by the larger construction energy costs of denitrifiers.

Oxidation of Ammonia and Reduction of Oxygen by Nitrifiers

Constraints on nitrifier oxidation of NH_3 imposed by O_2 uptake are solved in four steps:

1) substrate (NH_3) oxidation under non-limiting O_2 is calculated from active biomass, NH_3 and CO_2 concentrations, and an Arrhenius function of T_s [H11],

2) O_2 reduction to H_2O under non-limiting O_2 is calculated from 1) using set respiratory quotients [H12],

3) O_2 reduction to H_2O under ambient O_2 is calculated from radial O_2 diffusion through water films of thickness determined by soil water potential [H13a] coupled with active uptake at nitrifier surfaces driven by 2) [H13b]. O_2 uptake by nitrifiers also accounts for competition for O_2 uptake with heterotrophic DOC oxidizers, roots and mycorrhizae,

4) NH_3 oxidation to NO_2- under ambient O_2 is calculated from 2) and 3) [H14]. The energy yield of NH_3 oxidation drives the fixation of CO_2 for construction of microbial biomass $M_{i,n}$ according to construction energy costs of nitrifier populations.

Oxidation of Nitrite and Reduction of Oxygen by Nitrifiers

Constraints on nitrifier oxidation of NO_2^- to NO_3^- imposed by O_2 uptake [H15 - H18] are solved in the same way as are those of NH_3 [H11 - H14]. The energy yield of NO_2^- oxidation drives the fixation of CO_2 for construction of microbial biomass $M_{i,o}$ according to construction energy costs of each nitrifier population.

Oxidation of Ammonia and Reduction of Nitrite by Nitrifiers

Constraints on nitrifier oxidation of NH_3 imposed by NO_2^- availability are solved in three steps:

1) NO_2^- reduction to N_2O under non-limiting NO_2^- is calculated from electrons demanded by NH_3 oxidation but not accepted for O_2 reduction to H_2O because of diffusion limitations to O_2 supply, and hence transferred to NO_2^- [H19],
2) NO_2^- reduction to N_2O under ambient NO_2^- and CO_2 is calculated from 1) [H20], competing for NO_2^- with denitrifiers [H8] and nitrifiers [H18],
3) additional NH_3 oxidation to NO_2^- enabled by NO_2^- reduction in 2) [H21] is added to that enabled by O_2 reduction from [H14]. The energy yield from this oxidation drives the fixation of additional CO_2 for construction of $M_{i,n}$.

Uptake of Ammonium and Reduction of Oxygen by Roots and Mycorrhizae

1) NH_4^+ uptake by roots and mycorrhizae under non-limiting O_2 is calculated from mass flow and radial diffusion between adjacent roots and mycorrhizae [C23a] coupled with active uptake at root and mycorrhizal surfaces [C23b]. Active uptake is subject to inhibition by root nonstructural N:C ratios [C23g] where nonstructural N is the active uptake product, and nonstructural C is the CO_2 fixation product transferred to roots and mycorrhizae from the canopy.
2) O_2 reduction to H_2O is calculated from 1) plus oxidation of root and mycorrhizal nonstructural C under non-limiting O_2 using a set respiratory quotient [C14e],
3) O_2 reduction to H_2O under ambient O_2 is calculated from mass flow and radial diffusion between adjacent roots and mycorrhizae [C14d] coupled with active uptake at root and mycorrhizal surfaces driven by 2) [C14c]. O_2 uptake by roots and mycorrhizae also accounts for competition with O_2 uptake by heterotrophic DOC oxidizers, and autotrophic nitrifiers, calculated from their O_2 demands relative to those of other populations.
4) oxidation of root and mycorrhizal nonstructural C to CO_2 under ambient O_2 is calculated from 2) and 3) [C14b],
5) NH_4^+ uptake by roots and mycorrhizae under ambient O_2 is calculated from 1), 2), 3) and 4) [C23b].

Cation Exchange and Ion Pairing of Ammonium

A Gapon selectivity coefficient is used to solve cation exchange of NH_4^+ vs. Ca^{2+} [E10] as affected by other cations [E11] – [E15] and CEC [E16]. A solubility product is used to equilibrate soluble NH_4^+ and NH_3 [E24] as affected by pH [E25] and other solutes [E26 – E57].

Soil Transport and Surface - Atmosphere Exchange of Gaseous Substrates and Products

Exchange of all modelled gases γ (γ = O_2, CO_2, CH_4, N_2, N_2O, NH_3 and H_2) between aqueous and gaseous states is driven by disequilibrium between aqueous and gaseous concentrations according to a T_s-dependent solubility coefficient, constrained by a transfer coefficient based on air-water interfacial area that depends on air-filled porosity [D14 – D15] (Fig. 1). These gases undergo convective-dispersive transport through soil in gaseous [D16] and aqueous [D19] states driven by soil water flux and by gas concentration gradients. Dispersive transport is controlled by gaseous diffusion [D17] and aqueous dispersion [D20] coefficients calculated from gas- and water-filled porosity. Exchange of all gases between the atmosphere and both gaseous and aqueous states at the soil surface are driven by atmosphere - surface gas concentration differences and by boundary layer conductance above the soil surface, calculated from wind speed and from structure of vegetation and surface litter [D15].

FIELD EXPERIMENT

Site description

The Oensingen field site is located in the central Swiss lowlands (7° 44'E, 47° 17'N) at an altitude of 450 m. The climate is temperate with an average annual rainfall of about 1100 mm and a mean air temperature of 9.5 °C. The soil is classified as a Eutri-Stagnic Cambisol developed on clayey alluvial deposits, key properties of which are given in Table 1. Prior to the experiment, the field site was managed as a ley-arable rotation. In December 2000, the field was ploughed and left in fallow until 11 May 2001. The field was then sown with a grass-clover mixture typical for permanent grassland under intensive management. The field was ploughed again on 19 December 2007, left in fallow until 5 May 2008, when it was tilled and re-sown with the same grass-clover mix as in 2001. The period of study extended from sowing in 2001 to the end of 2009, during which the field was cut between three and five times per year and harvested as hay, silage or fresh grass, fertilized two to three times per year with manure as liquid cattle slurry and two to three times per year with mineral fertilizer as

ammonium nitrate (NH_4NO_3) pellets, for an average annual N application of 23 g N m^{-2}. All key management operations during this period are summarized in Table 2.

Soil, plant and meteorological measurements

Soil θ and T_s were recorded continuously using TDR (Time Domain Reflectometry, ThetaProbe ML2x, Delta-T Devices, Cambridge, UK) and thermocouples at 5, 10, 30 and 50 cm for θ and at 2, 5, 10, 30 and 50 cm for T_s. Leaf area index (LAI) was measured weekly with an optical leaf area meter (LI-2000, Li-Cor, Lincoln, NB, USA). Plants were collected every 2 to 4 weeks and the samples were dried for 48 h at 80°C, weighed and analyzed for C, N, P and K by using an elemental analyzer. Hourly climatic data were recorded continuously with an automated meteorological station, including air temperature (°C), rainfall (mm), relative humidity (%), global radiation (W m^{-2}) and windspeed (m s^{-1}).

Nitrous oxide flux measurements

N_2O fluxes were measured with a fully automated system consisting of up to eight stainless steel chambers (30 cm × 30 cm × 25 cm) (Flechard et al., 2005, Felber et al., 2014) fixed on PVC frames permanently inserted 10-cm deep into the soil. The positions of the chambers were changed about every two months. During measurements, the lids of the chambers were sequentially closed for 15 min. every 2 hours to allow N_2O accumulation in the chamber headspace. During closure the chamber atmosphere was recirculated at a rate of 1000 ml $min.^{-1}$ through polyamide tube lines (4-mm ID) to analytical instruments installed in a temperature-controlled field cabin adjacent to the field plots (10 m) and then back to the chamber headspace. Until autumn 2006 concentrations of N_2O, CO_2 and H_2O in the head space were measured once per minute with an INNOVA 1312 photoacoustic multi-gas analyzer (INNOVA Air Tech Instruments, Ballerup, Denmark; www.innova.dk). Interferences in the measurements caused by overlaps in the absorption spectra of the different gases and by temperature effects were corrected with a calibration algorithm described in detail by Flechard et al (2005). In autumn 2006 the system was changed to the gas filter correlation technique for N_2O (Model 46C, Thermo 279 Environmental Instruments Inc., Sunnyvale, CA, USA). This system was calibrated every 8 hours using certified standard gas mixtures (Messer Schweiz AG, Lenzburg, Switzerland) (Felber et al. 2014).

These measurements were used to calculate N_2O fluxes from the rate of change in concentration by using a linear or non-linear approach determined by the HMR R-package (Pedersen et al., 2010). The first three of the fifteen 1-min. measurements were omitted from the flux calculation to exclude gas exchange during closing that did not result from changes in emission/production in the soil. This procedure caused a mean increase of about 30% in the fluxes compared to values published in Fléchard et al. (2005) and Ammann et al. (2009), which were evaluated using linear regression. Fluxes from all chambers were averaged over 4-hourly intervals and resulting values attributed to the mid-points of the intervals. Standard errors of these averages were calculated from all fluxes measured during each interval, and thus included both spatial and temporal variation. The fluxes measured from 2002 to 2003 were summarized in Fléchard et al. (2005). Those from 2004 to 2007 were re-evaluated from values described in Ammann et al. (2009). Those from 2008 and 2009 were reprocessed from the EU-Project NitroEurope-IP database using the HMR algorithm.

CO_2 and Energy Flux Measurements

CO_2 and energy fluxes were measured by an eddy covariance (EC) system consisting of three-axis sonic anemometers (models R2 and HS, Gill instruments, Lymington, UK) and an open-path infrared CO_2/H_2O gas analyzer (model LI-7500, Li-Cor, Lincoln, USA). The EC system used in this study is described in Ammann et al. (2007). The EC tower was located in the centre of the field (52m x 146m), whereas the chambers were located in the south east corner. For most meteorological conditions, the chambers were not within the footprint of the EC towers, although for the main wind directions 80% or more of the footprint was within the field (Neftel et al. 2008). The management of the entire field was uniform throughout the experiment.

MODEL EXPERIMENT

Ecosys was initialized with the biological properties of plant functional types (PFTs) representing the ryegrass and clover planted at Oensingen. These properties were identical to those in an earlier study (Grant et al., 2012) except for a perennial rather than annual growth habit. These PFTs competed for common resources of radiation, water and nutrients, based on their vertical distributions of leaf area and root length driven by uptake and allocation of C, N and P in each PFT. *Ecosys* was also initialized with the physical and chemical properties of the Eutri-Stagnic Cambisol at Oensingen (Table

353 1). The model was then run from model dates 1 Jan. 1931 to 31 Dec. 2000 under repeating sequences of
354 land management practices and continuous hourly weather data (radiation, T_a, RH, wind speed and
355 precipitation) recorded at Oensingen from 1 Jan. 2001 to 31 Dec. 2007 (i.e. 10 cycles of 7 years). This
356 run was long enough for C, N and energy cycles in the model to attain equilibrium under the Oensingen
357 site conditions well before the end of the spinup run. The modelled site was plowed on 19 Dec. 2000,
358 terminating all PFTs.

359 The model run was then continued from model dates 1 Jan. 2001 to 31 Dec. 2009 under
360 continuous hourly weather data recorded at Oensingen from 1 Jan. 2001 to 31 Dec. 2009 with the
361 same PFTs and land management practices as those at the field site listed in Table 2. For each manure
362 application in the model, an irrigation of 4 mm was added to account for the water in the slurry. For
363 each harvest in the model, the fraction of canopy LAI to be cut (usually 0.85 – 0.95) was calculated
364 from measurements of LAI before and after the corresponding harvest in the field. In *ecosys*, leaves of
365 each PFT are aggregated into a common canopy which is dynamically resolved into a selected
366 number of layers (10 in this case) of equal LAI for calculating irradiance interception. The leaf
367 fraction to be cut was removed from successive leaf layers from the top of the combined canopy
368 downwards until the cumulative removal attained the set fraction, so that the LAI cut from each PFT
369 depended on the leaf area of the PFT in these layers. Of the phytomass cut with the LAI, 0.76 was
370 removed as harvest and the remainder was added to surface litter, as determined in the intensively
371 managed grassland at Oensingen by Amman et al. (2009). N_2O emissions modelled from 2004
372 through 2009 were compared with those measured by the automated chambers by regressing log-
373 transformed 4-hour averages of modelled on measured values during each year of the study, and also
374 by regressing total emissions modelled vs. measured during emission events following each fertilizer
375 or manure application. These comparisons were supported by ones with thermistor and TDR
376 measurements of T_s, θ, and with EC measurements of CO_2 and energy exchange.
377

378 **Model Sensitivity Studies**

379 Modelled N_2O emissions may be affected by three general sources of uncertainty in model
380 inputs: land management practices, soil properties and model parameters. To examine the possible
381 effects of some different land management practices on N_2O emissions, the model run from 2001 to
382 2009 (field) was repeated with (1) increased harvest intensity in which canopy LAI remaining after
383 each harvest was reduced to one-half of those in the first run (1/2), and (2) increased harvest intensity

with each harvest delayed by 5 days (1/2 + 5d). These alternative practices caused canopy regrowth and hence N uptake to be slower during emission events following subsequent manure and fertilizer applications.

To examine the possible effects of spatial variability in soil properties on N_2O emissions, the model run from 2001 to 2009 (field) was repeated with bulk density (BD) of the upper 3 cm in the soil profile (Table 1) increased by 5% or 10%. These larger BDs reduced soil porosity in the upper 3 cm of the soil, thereby slowing gas exchange with the atmosphere, particularly when the soil was wet (Fig. 1). All other soil properties used in the model remained unchanged (Table 1).

To examine an effect of uncertainty in model parameterization, the model run from 2001 to 2009 (field) was repeated with the values of two key parameters governing N_2O emissions, the Michaelis-Menten constants for reduction of O_2 (K_{O_2} in [H4]) or of NO_3^- and NO_2^- (K_{NO_x} in [H7], [H8] and [H20]), halved or doubled from those used in the model. Halving or doubling K_{O_2} hastened or slowed the reduction of O_2 by nitrifiers and denitrifiers and hence slowed or hastened the transfer of electrons to reduce NO_2^- and NO_3^- during nitrification and denitrification. Halving or doubling K_{NO_x} hastened or slowed the reduction of NO_2^- by nitrifiers and of NO_3^- and NO_2^- by denitrifiers All other parameters in the model remained unchanged.

RESULTS

LAI Modelled vs. Measured from 2002 to 2009

Accurate modelling of ecosystem C cycling and hence N_2O emissions requires accurate modelling of plant growth as determined by land management practices. LAI modelled and measured from 2002 to 2009 rose rapidly from low values remaining in spring and after each harvest (Table 1) to 4 – 6 m^2 m^{-2} before the next harvest, except during 2003 (Fig. 2). Regrowth of LAI in *ecosys* was driven by plant nonstructural C, N and P pools replenished from storage reserves remobilized after harvests, and from products of current C, N and P uptake, those of C being governed by irradiance interception calculated from regrowing LAI. Regrowth in the model was less rapid than that measured in 2009 (Fig. 2) because more frequent cutting forced more frequent replenishment of plant

nonstructural C, N and P pools which gradually depleted storage reserves and hence slowed subsequent regrowth. Hence rates of regrowth modelled after harvests were affected by harvest timing and intensity, as represented by the fractions of LAI removed at harvest.

N2O Fluxes Modelled vs. Measured from 2004 to 2009

During peak emissions, standard deviations of N_2O fluxes measured within each 4-hourly interval were found to be as much as 85% relative to mean values. These deviations were largely attributed to small-scale spatial variation in land management (manure and fertilizer application, surface litter from harvesting) and in soil properties (bulk density, water retention), which was not represented in the model run, rather than to temporal variation in environmental conditions (θ, T_s) which was represented in the model run. Therefore only a limited fraction of variation in the measured values was amenable to correlation with modelled values. Consequently slopes and coefficients of determination (R^2) from regressions of modelled on measured log-transformed fluxes varied from 0.5 to 1.0 and from 0.1 to 0.5 respectively, while intercepts remained close to zero (Table 3a). However ratios of mean squares for regression vs. error (F) were highly significant ($P < 0.001$) in all years of the study, indicating some agreement in the timing and magnitude of modelled and measured emission events. Improved agreement would require that more detailed information about land management and soil properties at each chamber site be provided to the model.

Daily-Aggregated N_2O Fluxes Modelled vs. Measured from 2004 to 2009

Daily aggregations of both measured and modelled N_2O emissions indicated that emission events during the study period were confined to intervals of no longer than 5 days when precipitation followed manure or fertilizer applications (Fig. 3). Outside of these intervals emissions remained very small except for a period of emissions modelled, but not measured, after manure application in autumn 2006 (Fig. 3c) and measured, but not modelled, before fertilizer application in spring 2008 (Fig. 3e).

The largest emissions followed manure applications in July and August, but their magnitudes did not vary with the amount of manure N applied. For example, emissions during an event in August 2009 (244 vs. 185 mg N m^{-2} measured vs. modelled in Fig. 3f) were greater than those during an event in July 2007 (86 vs. 112 mg N m^{-2} measured vs. modelled in Fig. 3d) which in turn were greater

446 than those during an event in July 2005 (54 vs. 96 mg N m^{-2} measured vs. modelled in Fig.2b).
447 However manure N application preceding the event in August 2009 (4.5 g N m^{-2}) was less than that in
448 July 2007 (6.7 g N m^{-2}) which in turn was less than that in July 2005 (8.5 g N m^{-2}) (Table 2), so that
449 smaller applications were followed by greater emissions, precluding a simple emission factor for
450 manure N application.
451
452 The magnitude of emission events following fertilizer application also varied. For example,
453 emissions during an event in late August 2007 (105 vs. 82 mg N m^{-2} measured vs. modelled in Fig.
454 3d) were greater than those during events in September 2004 (24 vs. 2 mg N m^{-2} measured vs.
455 modelled in Fig 2a) and 2005 (6 vs. 11 mg N m^{-2} measured vs. modelled in Fig. 3b), although the
456 fertilizer N applications of 3.0 g N m^{-2} preceding each event were the same (Table 2). These
457 differences in emissions indicated important differences in ecological controls imposed by
458 environmental conditions (θ and T_s) and plant management during each event.
459
460 The standard deviations of ~85% relative to the mean values of fluxes measured within each 4-
461 hourly interval during emission events was used to estimate an uncertainty in daily-aggregated fluxes
462 of *ca*. 30%. Uncertainty in daily fluxes measured during emission events was smaller than the several-
463 fold differences among the events indicating that the magnitude of these events likely differed
464 significantly. Regressions of modelled on measured total emissions during the events following each
465 fertilizer or manure application from 2004 to 2009 (Fig. 3) gave better agreement than did those of the
466 4-hourly averaged fluxes (Table 3b), indicating that modelling the precise timing of fluxes during
467 these events remains a challenge.
468
469 **Relationships between N_2O Fluxes and Environmental Conditions during Selected Emission**
470 **Events**
471 Environmental conditions measured and modelled from harvest to the end of the two largest
472 emission events following manure applications in July 2007 (Fig. 3d) and August 2009 (Fig. 3f) were
473 examined in greater detail to investigate relationships among near-surface T_s, θ, aqueous gas
474 concentrations, and surface fluxes of energy, CO_2 and N_2O (Figs. 4 and 5). In July 2007, several small
475 precipitation events wetted and cooled the soil between harvesting on DOY 187 and manure
476 application on DOY 194 (Fig. 4a,b). The soil then dried during several days without precipitation and

477 warmed with reduced shading from defoliation (Fig. 2) until DOY 200, after which the soil wetted
478 with further precipitation and cooled with increased shading from plant regrowth (Fig. 4a,b). The
479 higher θ measured during this period (Fig. 4b) may have been caused by difficulties in maintaining
480 calibration of the TDR probes over long periods in the high-clay soil at Oensingen (Table 1). This
481 higher θ was not likely caused by overestimated evapotranspiration because modelled LE fluxes,
482 reduced by low LAI after harvesting but increasing with subsequent regrowth, were close to those
483 measured (Fig. 4c), suggesting that total water uptake was accurately modelled. Comparison of
484 modelled and measured θ was further complicated by soil cracking which altered infiltration at low θ.
485 The effects of θ–dependent macroporosity on preferential flow are explicitly modelled in *ecosys*, but
486 have not yet been tested in detail.
487
488 CO_2 influxes were also reduced by low LAI after cutting, but recovered to pre-cut levels by the
489 end of the emission event (Fig. 4d), driving rapid regrowth of LAI (Fig. 2). Large CO_2 effluxes
490 measured and modelled after manure application indicated rapid R_h and hence O_2 demand that
491 persisted for several days.. Influxes measured in the field were reduced from those in the model for
492 several days after manure application, suggesting temporary interference of CO_2 fixation by the
493 manure application which was not accounted for in the model.
494
495 Litterfall from plant growth [C18, C19] and cutting, as well as from manure application caused
496 a litter layer of 1 – 2 cm to develop on the soil surface in the model. During the N_2O emission event
497 from DOY 200 to DOY 205 in 2007 (Fig. 3d), several precipitation events (Fig. 4a) wetted the
498 modelled surface litter and near-surface soil (layers 1 and 2 in Table 1) (Fig. 4e) without increasing θ
499 at 5 cm (Fig. 4b). This surface wetting slowed gas exchange with the atmosphere, sharply reducing
500 aqueous O_2 concentrations [$O_{2(s)}$] (Fig. 4f) and thereby raising aqueous N_2O concentrations [$N_2O_{(s)}$]
501 (Fig. 4g). Between precipitation events, drying of the surface litter and near-surface soil in the model
502 allowed recovery of [$O_{2(s)}$] and forced declines in [$N2O_{(s)}$]. These rises and declines in [$N2O_{(s)}$] drove
503 rises and declines in N_2O emissions that tracked those measured in the chambers (Fig. 4h). These
504 emissions rose immediately with the onset of precipitation on DOY 200 (Fig. 4a) before wetting
505 occurred at 5 cm (Fig. 4b), indicating that emissions were driven by surface wetting (Fig. 4e)
506 combined with rapid O_2 demand (Fig. 4d). The net generation of N_2O modelled in each soil zone,
507 calculated from [H8] + [H20] – [H9], indicated that 0.21 of surface emissions originated in the surface

litter and the remainder in the 0 – 1 cm soil layer as indicated by higher [$N_2O_{(s)}$] (Fig. 4g), while the deeper soil layers were a very small net sink of N_2O. Rises and declines in [$N_2O_{(s)}$] also drove rises and declines in N_2 emissions that persisted until DOY 205, after which more rapid mineral N uptake with recovering plant growth, driven by rising LAI (Fig. 2) and hence CO_2 influxes (Fig. 4d), caused both emissions to return to background levels (Fig. 4h).

In 2009, a period of low precipitation with soil drying and warming occurred between harvesting in late July and manure application on DOY 218 in early August, followed by heavy precipitation with soil wetting and cooling on DOY 220 (Fig. 5a,b). LE effluxes and CO_2 influxes declined sharply with LAI after cutting, and did not recover to pre-cut levels by the end of the subsequent emission event on DOY 224 (Fig. 5c,d), indicating a slow recovery of plant growth. Slurry application caused brief surface wetting on DOY 218 (Fig. 5e) and heavy precipitation on DOY 220 caused prolonged soil wetting at the surface (Fig. 5e) and at 5 cm (Fig. 5b). Wetting caused declines in [$O_{2(s)}$] (Fig. 5f) and thereby rises in [$N_2O_{(s)}$] (Fig. 5g) that were sustained over 3 days. These rises drove particularly rapid N_2O emissions in the model which were consistent in magnitude with those measured in the chambers (Fig. 5h). Diurnal variation modelled with soil warming and cooling (Fig. 5a) was not apparent in the measurements, although modelled values remained within the large uncertainty of the measured values during the emission event. These large emissions were enabled in the model by slow plant uptake of manure N (Table 2) caused by the slow recovery of plant CO_2 uptake and hence growth after cutting (Fig. 5d). The rises in [$N_2O_{(s)}$] also drove rises in modelled N_2 emissions (Fig. 5h). Emissions declined with surface litter drying on DOY 223 (Fig. 5e) which allowed surface [$O_{2(s)}$] to rise (Fig. 5f) and [$N_2O_{(s)}$] to fall (Fig. 5g) while θ at 5 cm remained high (Fig. 5b), again indicating that N_2O emissions were largely determined by ecological controls in the surface litter and soil. The net generation of N_2O modelled in each soil zone indicated that 0.48 of surface emissions originated in the surface litter, 0.48 in the 0 – 1 cm soil layer and 0.05 in the 1 – 3 cm soil layer, while the deeper soil layers were a very small net sink of N_2O, as indicated by near-surface gradients of [$N_2O_{(s)}$] (Fig. 5g).

Greater N_2O emissions were modelled and measured during the event in August 2009 than in July 2007 (Fig. 5h vs. Fig. 4h), in spite of smaller N addition (Fig. 3f vs. Fig. 3d; Table 2) and similar θ and T_s modelled and measured at 5 cm (Fig. 5a,b vs. Fig. 4a,b). These greater emissions were

539 attributed in the model to (1) earlier and heavier precipitation after manure application (2 days after
540 application in Fig. 5a vs. 6 days in Fig. 4a), and (2) slower recovery of CO_2 fixation after defoliation,
541 indicated by slower rises in diurnal amplitude of CO_2 fluxes (Fig. 5d vs. Fig. 4d). Heavier
542 precipitation in 2009 vs. 2007 drove sustained vs. intermittent surface and near-surface wetting (Fig.
543 5e vs. Fig. 4e) and hence sustained vs. intermittent declines in $[O_{2(s)}]$ and rises in $[N_2O_{(s)}]$ (Fig. 5f,g
544 vs. Fig. 4f,g). Slower recovery of CO_2 fixation after cutting in 2009 vs. 2007 slowed removal of added
545 NH_4^+ and NO_3^- from soil. This slower removal, combined with the shorter period between manure
546 application and precipitation, left larger NO_3^- concentrations ($[NO_3^-]$) in litter and surface soil to drive
547 N_2O production following precipitation [H7]. These model findings indicated the importance to N_2O
548 emissions of surface and near-surface θ after precipitation, and of plant management (intensity and
549 timing of defoliation in relation to N application) and its effect on subsequent plant CO_2 fixation and
550 N uptake.
551
552 **Effects of Intensity and Timing of Defoliation on N_2O Emission Events**
553 Increasing harvest intensity and delaying harvest dates slowed LAI regrowth modelled after
554 harvests (Fig. 6). The effects of this slowing on N_2O emissions during selected events modelled after
555 subsequent fertilizer and manure applications were examined under diverse θ and T_s (Figs. 7, 8).
556 Following manure application on DOY 194 in 2006 (Table 2), slower LAI regrowth from increasing
557 and delaying defoliation slowed the recovery of CO_2 fixation (Fig. 7a) and of NH_4^+ uptake (Fig. 7b),
558 allowing more nitrification of manure N and hence greater surface $[NO_3^-]$ (Fig. 7c). Slower LAI
559 regrowth (Fig. 6) also reduced shading and ET, raising T_s (Fig. 7d) and θ (Fig. 7e). N_2O emissions
560 modelled under field management remained small because of soil drying, in spite of high T_s,
561 consistent with measurements (Fig. 3c, Fig. 7f). Increases in emissions modelled with slower LAI
562 regrowth, particularly from delayed harvesting (Fig. 7f), were attributed to slower N uptake (Fig. 7b)
563 and hence larger $[NO_3^-]$ in litter and surface soil (Fig. 7c), and to warmer and wetter soil (Fig. 7d,e)
564 which increased O_2 demand while reducing O_2 supply.
565
566 Following a similar manure application on DOY 194 in 2007 (Table 2; Fig. 6), slower LAI
567 regrowth from increasing and delaying defoliation also caused reductions in CO_2 fixation (Fig. 7g),
568 which slowed NH_4^+ and NO_3^- uptake (Fig. 7h), allowing more nitrification of manure N and hence
569 greater $[NO_3^-]$ (Fig. 7i). Lower LAI also caused increases in T_s (Fig. 7j) and θ (Fig. 7k). Emissions

570 modelled and measured under field management in 2007 (Fig. 7l) were greater than those in 2006
571 (Fig. 7f), in spite of lower T_s (Fig. 7j vs. Fig. 7d), because near-surface wetting from several
572 precipitation events (Fig. 4a,e) reduced [$O_{2(s)}$] and increased [$N_2O_{(s)}$] (Fig. 4f,g). Emissions modelled
573 with increased and delayed harvesting rose from those with field harvesting as the emission event
574 progressed (Fig. 7l) because elevated [NO_3^-] from the manure application persisted longer during the
575 event (Fig. 7i).
576
577 Following fertilizer application on DOY 259 in 2005 (Table 2), modelled and measured
578 emissions remained small after soil wetting (Fig. 8f) because lower T_s (Fig. 8d) slowed soil
579 respiration after wetting, manifested as smaller measured and modelled CO_2 effluxes (Fig. 8a), and so
580 slowed demand for e^- acceptors. Under these conditions, increasing and delaying defoliation had little
581 effect on modelled N_2O emissions (Fig. 8f), while CO_2 fixation (Fig. 8a) and N uptake (Fig. 8b) were
582 only slightly reduced and surface NO_3^- only slightly increased (Fig. 8c). Following the same fertilizer
583 application on DOY 240 in 2007, modelled and measured emissions were greater than those in 2005
584 (Fig. 8l) because soils were warmer (Fig. 8j) with more rapid respiration (Fig. 8g), and because
585 fertilizer application and subsequent wetting occurred sooner after cutting (Table 2). Consequently
586 recovery of CO_2 fixation was less advanced (Fig. 8g), reducing cumulative N uptake (Fig. 8h) and
587 leaving larger [NO_3^-] to drive N_2O generation during the event (Fig. 8h). However reducing LAI
588 remaining after each harvest did not raise N_2O emissions after this application (Fig. 8l), because
589 slower LAI regrowth from earlier harvests had reduced primary productivity and consequently
590 litterfall and hence the mass of the surface litter from which much of the emitted N_2O was generated.
591 Consequently more intense harvests could cause surface litter later in the year to decline to levels at
592 which N_2O generation modelled in the litter was reduced.
593
594 **Annual Productivity, N_2O Emissions and the Effects of Defoliation Intensity and Timing**
595 In the model, plant management practices affected LAI regrowth (Fig. 6), CO_2 fixation, N
596 uptake, and hence soil [NO_3^-] and N_2O emissions (Figs. 7,8). These effects were summarized at an
597 annual time scale in Table 4. Modelled and EC-derived gross primary productivity (GPP) remained
598 close to 2000 g C m^{-2} y^{-1} during most years except with low precipitation in 2003 and replanting in
599 2008, indicating a highly productive ecosystem with rapid C cycling and hence rapid demand for e^-
600 acceptors (Table 4). Larger modelled vs. measured GPP caused larger modelled vs. measured NEP in

601 2003, 2005 and 2007. Harvest removals in the model varied with NEP except during replanting in
602 2008, but tended to exceed those recorded in the field, particularly with low EC-derived NEP in 2005
603 and 2006. Modelled values were determined in part by the assumed constant harvest efficiency of
604 0.76. Including C inputs from manure applications, modelled and estimated net biome productivity
605 (NBP) were positive except during replanting in 2008, indicating that this intensively managed
606 grassland was a C sink unless replanted. Average annual NBP modelled vs. measured from 2002 to
607 2009 was 30 vs. 58 g C m^{-2}, with the lower modelled value attributed to greater modelled harvest
608 removals, particularly in 2006.
609
610 Slower LAI regrowth from increasing and delaying defoliation (Fig. 6) reduced modelled GPP,
611 R_e and hence NEP by 5 - 10% during years with greater productivity. However increasing and
612 delaying defoliation did not much affect harvest removals because reduced NEP was offset by greater
613 harvest intensity, so that NBP was reduced except with replanting in 2008.
614
615 Annual N_2O emissions were estimated from chamber measurements for each year of the study
616 by scaling the mean measured fluxes to annual values. These values are presented in Table 4 as upper
617 boundaries for annual emissions because flux measurements from which means were calculated were
618 more frequent during emission events. A lower boundary for annual emissions was also estimated in
619 Table 4 by replacing missing flux measurements with zero. Average lower and upper boundaries for
620 annual emissions estimated from 2002 to 2009 were 0.220 and 0.355 g N m^{-2} respectively vs. an
621 average annual emission in the model of 0.260 g N m^{-2} (Table 4). Modelled emissions were nearer to
622 upper boundaries during years with lower measured emissions (2003, 2004, 2006), and to lower
623 boundaries during years with higher measured emissions (2007, 2008, 2009). There was no significant
624 correlation between annual N inputs and measured or modelled emissions. Although annual emissions
625 in the model were close to 1% of annual N inputs during most years, they were greater in 2008 and
626 2009 in spite of smaller N inputs because of the large emission events modelled after summer
627 applications of fertilizer and manure (Fig. 3e,f; Fig. 5h). Annual N inputs (Table 4), supplemented by
628 3 – 6 g N m^{-2} y^{-1} modelled from symbiotic fixation by clover [F1 – F26]), were only slightly larger
629 than annual N removals with harvesting, supplemented by losses of 2 – 3 g N m^{-2} y^{-1} from all other
630 gaseous and aqueous emissions (N_2 from denitrification, NH_3 from volatilization, NO_3^- from
631 leaching). Consequently residual soil NO_3^-, while present in the model, did not accumulate during the

study period, and so did not drive increasing N_2O emissions with sustained N applications. Modelled and measured annual N_2O emissions, if expressed in C equivalents (~130 g C g N^{-1}), largely offset net C uptake expressed as NBP (Table 4).

Increasing harvest intensity and delaying harvest dates had little effect on annual N_2O emissions modelled during the first two years after planting in 2001 and 2008, but raised them substantially thereafter (2003 – 2007) (Table 4). During this period, annual emissions rose by an average of 24% with increased harvest intensity, and by an average of 43% with increased harvest intensity combined with delayed harvest dates. These increases were attributed to reduced N uptake, and to increased T_s and θ (Figs. 7, 8).

Effects of increased bulk density on N_2O emissions

Increasing near-surface (0 – 3 cm) soil BD by 5% or 10% at the beginning of 2001 in the model reduced [$O_{2(s)}$] after rainfall events and slowed recovery of [$O_{2(s)}$] during subsequent drying as shown following the manure application in July 2007 (Fig. 9a) and the fertilizer application in late August 2007 (Fig. 9c). These reductions caused increases in modelled N_2O effluxes that varied during emission events (Fig. 9b,d). Effluxes modelled with increases of 10% in near-surface BD were at times double those modelled without (e.g. DOY 201 and 240 in Fig. 9), indicating that relatively small changes in soil surface properties could at times cause large changes in emissions. The effects of increased BD on modelled T_s, θ, CO_2 exchange, crop production and N uptake during these events were small (results not shown). Increasing near-surface BD by 10% raised annual N_2O emissions by amounts that increased with annual precipitation from *ca*. 10% in drier years (e.g. 2003) to *ca*. 50% in wetter (e.g. 2006) (Table 5).

Effects of Changes in K_{O_2} and K_{NO_x} on N_2O emissions

Lowering K_{O_2} to one-half that used in *ecosys* reduced annual N_2O emissions modelled from 2004 to 2009 by 16% to an average of 0.218 g N m^{-2} y^{-1}, near the average lower boundary of the measured values (Table 5). Raising K_{O_2h} to double that used *ecosys* increased these emissions by 28% to an average of 0.334 g N m^{-2} y^{-1}, near the average upper boundary of the measured values. Lowering K_{NO_x} to one-half that used in *ecosys* increased annual N_2O emissions modelled from 2004 to 2009 by 30% to an average of 0.338 g N m^{-2} y^{-1}, near the average upper boundary of the measured values

(Table 5). Raising K_{NO_x} to double that used *ecosys* reduced these emissions by 27% to an average of 0.189 g N m^{-2} y^{-1}, near the average lower boundary of the measured values. In years with lower annual emissions (2003, 2004, 2006 in Table 4), the lower K_{O_2} or higher K_{NO_x} gave modelled values that were closer to measured values. However in years with higher annual emissions (2008 and 2009 in Table 4), the higher K_{O_2} or lower K_{NO_x} gave modelled values that were closer.

DISCUSSION

Modelled vs. Measured N_2O Emissions

Most N_2O emission events measured from 2004 to 2009 were simulated within the range of measurement uncertainty, estimated to be about 30% of mean daily values (Fig. 3). However some deviations between modelled and measured N_2O emissions were apparent, such as the larger emissions modelled in autumn 2006 (Fig. 3c) and the smaller emissions modelled in spring 2008 (Fig. 3e). These deviations may be attributed to uncertainties in both the measurements and the model. In the automated measurement system, the static chambers were rotated about every two months among fixed positions in a corner of the field. During these periods, surface conditions in the chamber could deviate from the mean field conditions represented in the model. However we do not have an explanation for the very small emissions measured after the three manure slurry applications 2006. The chambers had been removed before the applications and were reinstalled within two hours, during which the cut grass was removed so that the surface litter in the chambers may have been reduced from that outside. In the model, emissions following manure or fertilizer applications were sensitive to the amount of surface litter as noted earlier. The absence of emission events measured after slurry applications in 2006 was unusual (Fig. 3) given the large precipitation that year (Table 4), demonstrating that large variability at small spatial scales inevitably affects these measurements. Such variability adversely affects agreement between modelled and measured emissions (Table 3).

During spring 2008 sustained emissions of about 5 mg N m^{-2} d^{-1} were measured by the chambers in the absence of any manure or fertilizer applications (Fig. 3e). These emissions were related to the ploughing of the field to a depth of 25cm in December 2007 (Table 2) which hastened soil organic matter decomposition, and hence N mineralization that increased mineral N substrate for

694 nitrification and denitrification, and possibly microbial nitrifier and denitrifier populations. These
695 increases must remain conjectural as the Oensingen study did not include stratified analysis of N_2O
696 production factors (e.g. microbial biomass, potential denitrification) within the chamber soils.
697 Although *ecosys* simulates hastened SOM decomposition with tillage (Grant et al., 1998), large
698 amounts of above- and below-ground plant litter with relatively high C:N ratios were incorporated in
699 the model with tillage in December 2007 which slowed net N mineralization and hence accumulation
700 of mineral N products in the model during spring 2008. Consequently modelled N_2O emissions
701 remained small until mineral N was raised by fertilizer applications in July (Fig. 3c).
702
703 **Modelling Controls on N_2O Emissions by Litter and Near-Surface θ and T_s**
704 In the model, almost all the N_2O emissions originated in the surface litter and in the near-
705 surface (0 – 1 cm) soil layer, so that emissions were strongly controlled by litter and near-surface θ
706 and T_s (Figs. 3 – 4). This model finding is consistent with the experimental finding of Pal et al. (2013)
707 from ^{15}N enrichment studies that approximately 70% of N_2O measured during emission events in a
708 managed grassland originated in the surface litter. Similarly van der Weerden et al. (2013) inferred
709 from diurnal variation in T_s and N_2O emissions measured after urine amendments on a managed
710 grassland that N_2O production was at or near the soil surface (0 - 2 cm). Also Fléchard et al. (2007)
711 inferred in a meta-analysis of N_2O emissions from grasslands in Europe that θ measured at 5 cm was
712 not in some cases an adequate scaling factor for N_2O source strength because N_2O production and
713 emission took place at or near the soil surface. *Ecosys* simulated little net production, and even a
714 small net consumption, of N_2O in soil below 2 cm during emission events, as may be inferred from
715 peak $[N_2O_{(s)}]$ modelled in the 0 – 1 cm soil layer and much lower $[N_2O_{(s)}]$ modelled in the 1 – 3 cm
716 soil layer below (Figs. 3g and 4g). This model finding was consistent with the experimental finding of
717 Neftel et al. (2000) that N_2O concentrations below near-surface soil layers in a managed grassland
718 remained below atmospheric values during emission events, from which they inferred that any N_2O
719 generated at depths greater than ~3 cm would not likely reach the soil surface. Thus attempts to relate
720 N_2O emissions to T_s and θ measured at greater depths than 3 cm in grasslands are unlikely to be
721 informative if these differ from near-surface values. These emissions should rather be related to
722 conditions in the litter and near-surface soil, which need to be better characterized in future studies.
723

Consequently modelled N_2O emissions were highly sensitive to surface wetting and drying (e.g. Fig. 4e,h) modelled from precipitation vs. ET (e.g. Fig. 4a,c), or to surface warming and cooling (e.g. Fig. 8j,l) modelled from surface energy balance (e.g. Fig. 4c). The sensitivity to surface wetting and drying was modelled from the effects of θ on air- vs. water-filled porosity and hence on diffusivity of gases in gaseous [D17] and aqueous [D20] phases, and on gaseous volatilization - dissolution transfer coefficients and hence gas exchange between gaseous and aqueous phases [D14, D15]. These transfers controlled O_2 supply, and hence demand for alternative e^- acceptors as the O_2 supply fell below O_2 demand, which drove N_2O generation from denitrification [H6 – H8] and nitrification [H19]. The control of O_2 supply on e^- acceptors used in nitrification thereby simulated the effect of WFPS on the fraction of N_2O generated during nitrification identified by Fang et al. (2015) as necessary to modelling N_2O emissions, while avoiding the model-specific parameterization needed in simpler models. The sensitivity to surface wetting in *ecosys* enabled sharp rises in N_2O emissions to be modelled from surface litter and near-surface soil after small precipitation events during DOY 200 - 201 in 2007 (Fig. 4a,h), and after slurry application during DOY 218 in 2009 (Fig. 5a,h), even when the soil at 5 cm remained dry (Fig. 4b; Fig. 5b). Such rises were consistent with the experimental findings of Fléchard et al. (2007) that precipitation on dry soil can cause substantial N_2O emissions after fertilizer application in grasslands.

The sensitivity to surface warming and cooling was modelled from the effects of T_s on diffusivity of gases in gaseous [D17] and aqueous [D20] phases, and on solubility of gases and hence exchange of gases between gaseous and aqueous phases [D14, D15], both parameterized from basic physical relationships independently from the model. These transfers controlled $[O_{2(s)}]$ in the surface litter and soil (Figs. 3f and 4f), and hence O_2 uptake by aerobic heterotrophs [H4] and autotrophs [H13] through a Michaelis-Menten constant [H4b, H13b]. The sensitivity to surface warming and cooling was also modelled from the effects of T_s on SOC oxidation [H2] and hence O_2 demand by aerobic heterotrophs [H3], and on NH_4^+ and NO_2^- oxidation [H11, H15] and hence O_2 demand by aerobic autotrophs [H12, H16]. These effects were driven by a single Arrhenius function used for all biological transformations [A6] parameterized from basic research conducted independently from the model. Under sustained high surface θ, this combination of physical and biological processes drove large diurnal variation in N_2O emissions modelled with diurnal surface warming and cooling during emission events (e.g. DOY 221 in Fig. 5h, DOY 243 in Fig. 8l), as observed experimentally by van

der Weerden et al. (2013). By explicitly simulating the diverse processes that determine N_2O emissions, *ecosys* could model the large sensitivity of emissions to T_s without the use of unrealistically large parameters for temperature sensitivity inferred from controlled temperature studies of N_2O emissions (e.g. Dobbie and Smith, 2001). This large sensitivity to T_s has been inadequately represented in simpler models, causing underestimation of large emissions measured from warm soils (e.g. Saggar et al., 2004). At a seasonal time scale, higher T_s could cause large increases in N_2O emissions modelled with comparable θ after the same fertilizer application (Fig. 8l vs. Fig. 8f). However the effects of T_s on N_2O emissions were dominated by those of θ during surface wetting and drying (e.g. Figs. 4h, 7l).

Values of both θ and T_s thus determined O_2 demand not met by O_2 uptake which drove demand for alternative e^- acceptors by heterotrophic denitrifiers [H6] and autotrophic nitrifiers [H19]. This demand drove the sequential reduction of NO_3^-, NO_2^- and N_2O to NO_2^-, N_2O and N_2 respectively by heterotrophic denitrifiers [H7, H8, H9], and the reduction of NO_2^- to N_2O by autotrophic nitrifiers [H20]. The consequent production of N_2O (Fig. 4g, Fig. 5g) and N_2 drove emissions of both N_2O and N_2 (Fig. 4h, Fig. 5h) through volatilization [D14, D15] and through gaseous and aqueous diffusion [D16, D19]. Ratios of N_2O and N_2 emissions in *ecosys* (Fig. 4h, Fig. 5h) were not parameterized as done in other models, but rather were determined by relative affinities determined from basic research [H8, H9], and by environmental conditions. When demand from heterotrophic denitrifiers for alternative e^- acceptors was small relative to their availability, the preferential reduction of more oxidized e^- acceptors generated larger emissions of N_2O [H7, H8] relative to N_2 [H9]. Such conditions occurred during the early part of an emission event when surface $[NO_3^-]$ rose with nitrification of fertilizer or manure NH_4^+ after application (e.g. DOY 200 – 201 in Fig. 4h). However when demand for alternative e^- acceptors was large relative to their availability, this same reduction sequence forced more rapid reduction of N_2O to N_2 and hence smaller emissions of N_2O relative to N_2. Such conditions occurred during the later part of emission events when surface $[NO_3^-]$ declined with plant uptake (e.g. DOY 202 – 205 in Fig. 4h and DOY 222 in Fig. 5h), or when greater surface wetting reduced O_2 supply (e.g. DOY 220 in Fig. 5h). This greater demand for alternative e^- acceptors with wetting provided a process-based explanation for declines in N_2O emissions frequently found at higher θ in field studies (e.g. Rafique et al., 2011) without explicit parameterization of N_2O:N_2 ratios.

Nitrification and denitrification were also driven by the concentrations of NH_4^+ [H11], NO_3^- [H7], NO_2^- [H8, H15, H20] and N_2O [H9] relative to Michaelis-Menten constants evaluated from basic research. The concentrations of NH_4^+ and NO_3^- in *ecosys* were increased by N additions from manure and fertilizer N applications (Table 2), and by net mineralization soil organic N from oxidation of litterfall, manure and SOM [A26] as indicated by soil CO_2 effluxes. These concentrations were reduced by root uptake of NH_4^+ and NO_3^- [C23] and consequent plant N assimilation with growth, indicated by more rapid CO_2 fixation with time after cutting (Figs 3 – 4 and Figs. 6 - 7). In the model, more rapid CO_2 fixation drove more rapid production of nonstructural C, and hence more rapid exchange of nonstructural C and N between canopy and roots [C50], and so hastened root active N uptake by increasing R_a driving root growth [C14b], and by hastening removal of N uptake products and hence reducing their inhibition of active uptake [C23g]. The diversity of controls on key substrates for N_2O generation suggests that robust simulations of N_2O emissions require comprehensive ecosystem models in which these controls are fully represented.

Modelling Effects of Defoliation Intensity and Timing on N_2O Emissions

The control of NH_4^+ and NO_3^- availability by root N uptake indicated that plant management practices determining uptake would thereby affect N_2O emissions. In the model, increasing harvest intensity and delaying harvest dates both slowed N uptake (Fig. 7b,h and Fig. 8b,h) by slowing the recovery of LAI (Fig. 6) and CO_2 fixation (Fig. 7a,g and Fig. 8a,g). Both thereby increased [NO_3^-] (Fig. 7c,i and Fig. 8c,i), T_s (Fig. 7d,j and Fig. 8d,j) and θ (Fig. 7e,k and Fig. 8e,k), raising N_2O effluxes modelled during most emission events (Fig. 7f,l and Fig. 8f,l), and hence annually (Table 4). This model finding was consistent with the field observations of Jackson et al. (2015) that increased N_2O emissions after defoliation in grasslands were caused by reduced uptake of N and water by slower-growing plants.

The effects of defoliation on N_2O emissions during modelled emission events were similar to, or greater than, those of T_s and θ (e.g. Fig. 7f,l), consistent with the experimental finding of Imer et al. (2013) that plant management, as represented by its effects on LAI, had a larger effect on N_2O fluxes than did the environment, as represented by T_a, at an intensively managed grassland in Switzerland. Reducing LAI remaining after harvest by one-half and delaying harvest by 5 days had little effect on modelled harvest removals (Table 4), suggesting that N_2O emissions from managed grasslands are

817 more sensitive to plant management practices than are yields. Intensity and timing of harvests should
818 therefore be selected to avoid slow regrowth of LAI following N additions by avoiding excessive
819 defoliation and by allowing as much time as possible between defoliation and subsequent fertilizer or
820 manure application. Neftel et al. (2010) reported enhanced N_2O emissions after cuts in managed
821 grassland and hypothesized that a simple mitigation option would be to optimize the timing of the
822 fertilizer applications. To our knowledge this option has not been systematically investigated.
823
824 **Modelling Effects of Soil Bulk Density on N_2O Emissions**
825 The small increases in near-surface BD included in this study were typical of those arising from
826 natural variation in soil properties or from compaction by vehicular traffic during field management
827 operations. In the model, these increases reduced soil porosity and hence gaseous diffusivity [D17]
828 which slowed O_2 uptake from the atmosphere [D15] and O_2 transfer through the soil profile [D16].
829 Consequent reductions in near-surface [$O_{2(s)}$] (Fig. 9a,c) slowed O_2 reduction by denitrifiers [H4] and
830 nitrifiers [H13], forcing more rapid e^- transfer to NO_3^- by denitrifers [H6] and to NO_2^- by nitrifiers
831 [H19] and hence more rapid emissions of N_2O following applications of manure (Fig. 9b) and fertilizer
832 (Fig. 9d).
833
834 In a study of soil compaction effects on N_2O emissions from a fertilized agricultural field in a
835 climate similar to that at Oensingen, Bessou et al. (2010) found that increasing the BD of the upper 30
836 cm of the soil profile by *ca*. 15% raised annual N_2O emissions measured with automated chambers by
837 at least 50% during each of two growing seasons. These rises were similar to those modelled with a
838 smaller increase in BD of the upper 3 cm during the wettest year of this study (Table 5). During
839 emission events, Bessou et al. (2010) measured peak fluxes from compacted soil that were double
840 those from uncompacted, as also modelled here (Fig. 9b,d).
841
842 The detailed algorithms from which *ecosys* was constructed enabled increases in N_2O
843 emissions from surface compaction to be simulated from specified changes to surface BD, a
844 measureable site characteristic, without further model parameterization. The marked increases in N_2O
845 emissions modelled with these increases in BD (Table 5) indicated that some of the large spatial
846 variation in these emissions commonly found in field measurements could arise from relatively small
847 variation in physical properties of near-surface soil. In future studies of N_2O emissions, near-surface

soil properties could be determined at each measurement site to establish the extent to which variation in these properties are associated with those in emissions.

Modelling Effects of K_{O_2} and K_{NO_x} on N_2O Emissions

The value of K_{O_2} used in *ecosys* (=2 μM) was taken from the upper range of values determined experimentally for intact cells of heterotrophic bacteria by Longmuir (1954). Halving or doubling K_{O_2} changed modelled N_2O emissions (Table 5) by amounts similar to uncertainty in measured emissions expressed as lower and upper boundaries of likely values (Table 4), although the doubled value of K_{O_2} was larger than those derived from experiments. The value of K_{NO_x} used in *ecosys* (=100 μM) was within the range of values determined experimentally by Yoshinari et al. (1977). As for K_{O_2}, halving or doubling K_{NO_x} changed modelled N_2O emissions (Table 5) by amounts similar to uncertainty in measured emissions expressed as lower and upper boundaries of likely values (Table 4). The halved value of K_{NO_x} was closer to those measured by Betlach and Tiedje (1981) and Khalil et al. (2007) while the doubled value was closer to that measured by Klemedtsson et al. (1977). These changes indicate that key parameters used in process models must be capable of being constrained by accurate evaluation in independent experiments.

CONCLUSIONS

N_2O emissions modelled in this managed grassland originated in the surface litter and upper 2 cm of the soil profile. The shallow origin of these emissions enabled *ecosys* to simulate the response of measured emissions to changes in near-surface θ and T_s during brief emission events when rainfall followed manure or mineral fertilizer applications. Measurements of θ and T_s used to estimate N_2O emissions from managed grasslands should therefore be taken in surface litter and near-surface soil (0 – 2 cm), rather than deeper in the soil profile (5 – 10 cm) as is currently done.

N_2O fluxes modelled during emission events were greater when grassland regrowth and hence mineral N uptake was slower following harvest and subsequent N application. The control of N_2O emissions by grassland N uptake indicated that N_2O emissions from managed grassland could be

878 increased by harvesting practices and fertilizer timing that resulted in slower regrowth during periods
879 when emission events are most likely to occur. N_2O fluxes modelled during emission events rose
880 sharply with small increases in surface BD, indicating the importance of avoiding surface compaction
881 in fields to which large amounts of N are applied.
882
883 The basic and comprehensive approach to model development in *ecosys* allowed diverse
884 responses of N_2O emissions to changes in weather (T_s, θ), land management and soil properties to be
885 modelled from specified changes to readily measured inputs with parameters constrained by basic
886 experiments conducted independently of the model rather than derived from site-specific observations.
887 This approach enabled concurrent, well-constrained tests of model performance against a diverse set of
888 field measurements, and so is expected to confer robustness to the modelling of these emissions under
889 different climates, soils and land uses in future studies.
890

891 ACKNOWLEDGEMENTS

892

893 Computational facilities for *ecosys* were provided by the University of Alberta and by the
894 Compute Canada high performance computing infrastructure. A PC version of *ecosys* with GUI can be
895 obtained by contacting the corresponding author at rgrant@ualberta.ca. The authors also acknowledge
896 contributions from valuable discussions with Christoph Amman concerning measurement methodology.

REFERENCES

Ammann, C., Fléchard, C., Leifeld, J., Neftel, A. and Fuhrer, J.:. The carbon budget of newly established temperate grassland depends on management intensity. Agriculture, Ecosystems and Environment 121, 5–20, 2007

Ammann, C., Spirig, C., Leifeld, J. and Neftel, A.: Assessment of the nitrogen and carbon budget of two managed temperate grassland fields. Agriculture, Ecosystems and Environment 133, 150–162, 2009

Bessou, C., Mary, B., Léonard, B., Ro u s s e l. M., Gréhan, E. and Gabrielle, B.: Modelling soil compaction impacts on nitrous oxide emissions in arable fields. Euro. J. Soil Sci., 61, 348–363, 2010.

Betlach, M.R. and Tiedje, J.M.: Kinetic explanation for accumulation of nitrite, nitric oxide, and nitrous oxide during bacterial denitrification. Appl. Environ Microbiol., 42, 1074-1084, 1981.

Chatskikh, D.D., Olesen, J.E., Berntsen, J., Regina, K. and Yamulki, S.: Simulation of effects of soils, climate and management on N_2O emission from grasslands, Biogeochem. 76, 395-419, 2005

Conant, R.T, Paustian, K., Del Grosso, S.J. and Parton, W.J.: Nitrogen pools and fluxes in grassland soils sequestering carbon. Nutr Cycl Agroecosyst 71, 239–248, 2005.

Craswell, E. T.: Some factors influencing denitrification and nitrogen immobilization in a clay soil, Soil Biol. Biochem. 10, 241-245, 1978

Dobbie, K.E. and Smith, K.A.: The effect of temperature, water-filled pore space, and land use on N_2O emissions from an imperfectly drained gleysol. Eur. J. Soil Sci. 52: 667–673, 2001

Fang, Q.X., Ma, L., Halvorson, A.D., Malone, R.W., Ahuja, L.R., Del Grosso, S.J. and Hatfield, J.L.: Evaluating four nitrous oxide emission algorithms in response to N rate on an irrigated corn field. Environmental Modelling & Software 72, 56-70, 2015.

Felber, R., Leifeld, J., Horak J and Neftel, A.: Nitrous oxide emission reduction with greenwaste biochar: comparison of laboratory and field experiments Euro. J. Soil Sci. 65, 128–138 doi: 10.1111/ejss.12093, 2014.

Fléchard, C.R., Neftel, A., Jocher, M., Ammann, C. and Fuhrer, J.: Bi-directional soil/atmosphere N_2O exchange over two mown grassland systems with contrasting management practices. Glob Change Biol 11, 2114–2127, 2005.

927 Fléchard, C.R., Ambus, P., Skiba, U., Rees, R.M., Hensen, A., van Amstel, A., van den Pol-van
928 Dasselaar, A., Soussana, J.-F., Jones, M., Clifton-Brown, J., Raschi, A., Horvath, L., Neftel, A.,
929 Jocher, M., Ammann, C., Leifeld, J., Fuhrer, J., Calanca, P., Thalman, E., Pilegaard, K., Di
930 Marco, C., Campbell, C., Nemitz, E., Hargreaves, K.J., Levy, P.E., Ball, B.C., Jones, S.K., van
931 de Bulk, W.C.M., Groot, T., Blom, M., Domingues, R., Kasper, G., Allard, V., Ceschia, E.,
932 Cellier, P., Laville, P., Henault, C., Bizouard, F., Abdalla, M., Williams, M., Baronti, S.,
933 Berretti F. and Grosz, B.: Effects of climate and management intensity on nitrous oxide
934 emissions in grassland systems across Europe, Agric. Ecosyst. Environ. 121, 135-152, 2007.
935 Grant, R.F."A review of the Canadian ecosystem model *ecosys*. pp. 173-264 in: *Modeling Carbon and*
936 *Nitrogen Dynamics for Soil Management*. Shaffer M. (ed). CRC Press. Boca Raton, F, 2001.
937 Grant, R.F. Baldocchi, D.D. and Ma, S.: Ecological controls on net ecosystem productivity of a
938 Mediterranean grassland under current and future climates. Agric. For Meteorol. 152: 189– 200,
939 2012.
940 Grant, R.F., Juma, N.G. and McGill, W.B.: Simulation of carbon and nitrogen transformations in soils. I.
941 Mineralization. Soil Biol. Biochem. 27, 1317-1329, 1993a
942 Grant, R.F., Juma, N.G. and McGill, W.B.: Simulation of carbon and nitrogen transformations in soils.
943 II. Microbial biomass and metabolic products. Soil Biol. Biochem. 27,1331-1338, 1993b
944 Grant, R.F., Izaurralde, R.C., Nyborg, M., Malhi, S.S., Solberg, E. D. and Jans-Hammermeister, D.:
945 Modelling tillage and surface residue effects on soil C storage under current vs. elevated CO_2
946 and temperature in *ecosys* pp. 527-547 in *Soil Processes and the Carbon Cycle*. Lal, R., Kimble
947 J.M., Follet, R.F. and Stewart, B.A.(eds). CRC Press. Boca Raton, FL, 1998.
948 Grant, R.F. and Pattey, E.: Mathematical modelling of nitrous oxide emissions from an agricultural field
949 during spring thaw. Global Biogeochem. Cycles. 13, 679-694, 1999
950 Grant, R.F. and Pattey E.: Modelling variability in N_2O emissions from fertilized agricultural fields. Soil
951 Biol. Biochem. 35, 225-243, 2003.
952 Grant, R.F. and Pattey, E.: Temperature sensitivity of N_2O emissions from fertilized agricultural soils:
953 mathematical modelling in *ecosys*. Global Biogeochem. Cycles 22, GB4019,
954 doi:10.1029/2008GB003273, 2008.
955 Grant, R.F., Pattey, E.M., Goddard, T.W., Kryzanowski, L.M. and Puurveen, H.: Modelling the effects
956 of fertilizer application rate on nitrous oxide emissions from agricultural fields. Soil Sci Soc.
957 Amer. J. 70, 235-248, 2006.

Imer, D., Merbold, L., Eugster, W. and Buchmann, N.: Temporal and spatial variations of soil CO_2, CH_4 and N_2O fluxes at three differently managed grasslands. Biogeosci. 10, 5931–5945, 2013.

Jackson, R.D., Oates, L.G., Schacht, W.H., Klopfenstein, T.J., Undersander, D.J., Greenquist, M.A., Bell, M.M. and Gratton, C.: Nitrous oxide emissions from cool-season pastures under managed grazing. Nutr Cycl Agroecosyst 101, 365–376, 2015.

Khalil, K., Renault, P.,. Guérin, N. and Mary, B.: Modelling denitrification including the dynamics of denitrifiers and their progressive ability to reduce nitrous oxide: comparisonwith batch experiments. Euro. J. Soil Sci. 56:491–504, 2005.

Klemedtsson, L., Svensson, B.H., Lindberg,T.and Rosswall,T.: The use of acetylene inhibition of nitrous oxide reductase in quantifying denitrification in soils. Swedish J. Agric. Res. 7, 179–185, 1977.

Longmuir, I.S.: Respiration rate of bacteria as a function of oxygen concentration. Biochem. 51, 81-87, 1954.

Li, Y., Chen, D., Zhang, Y., Edis, R. and Ding, H.: Comparison of three modeling approaches for simulating denitrification and nitrous oxide emissions from loam-textured arable soils, Global Biogeochem. Cycles 19, GB3002, doi:10.1029/2004GB002392, 2005

Leifeld, J., Ammann, C. Neftel, A. and Fuhrer, J.: A comparison of repeated soil inventory and carbon flux budget to detect soil carbon changes after conversion from cropland to grasslands. Global Change Biol. 17, 3366-3375, 2011

Lu, Y., Huang, Y., Zou, J. and Zheng, X.: An inventory of N_2O emissions from agriculture in China using precipitation-rectified emission factor and background emission, Chemosphere 65, 1915-1924, 2006.

Metivier, K.A., Pattey, E. and Grant, R.F.: Using the ecosys mathematical model to simulate temporal variability of nitrous oxide emissions from a fertilized agricultural soil. Soil Biol. Biochem. 41, 2370–2386, 2009.

Neftel, A., Blatter, A., Schmid, M., Lehmann, B. and Tarakanov, S.V.: An experimental determination of the scale length of N_2O in the soil of a grassland. J. Geophys. Res. 105, 12095–12103, 2000.

Neftel, A, Ammann, C., Fischer, F., Spirig, C., Conen, F., Emmenegger, L , Tuzson, B and Wahlen, S.: N_2O exchange over managed grassland: Application of a quantum cascade laser spectrometer for micrometeorological flux measurements Agric. For. Meteorol. 150, 775–785, 2010.

Neftel, A. Spirig, C. and Ammann, C.: Application and test of a simple tool for operational footprint evaluations. Environ. Poll. 152, 644-652, 2008

Pal, P., Clough, T.J., Kelliher, F.M. and. Sherlock, R.R: Nitrous oxide emissions from in situ deposition of 15N-labeled ryegrass litter in a pasture soil. J. Environ. Qual. 42, 323–331, 2013

Pedersen, A.R., Petersen, S.O. and Schelde, K.: A comprehensive approach to soil-atmosphere trace-gas flux estimation with static chambers. European Journal of Soil Science, 61, 888–902, 2010.

Rafique, R., Hennessy, D. and Kiely, G.: Nitrous oxide emission from grazed grassland under different management systems. Ecosystems 14: 563–582, 2011.

Ruzjerez, B.E., White, R.E. and Ball, P.R.: Long-term measurement of denitrification in three contrasting pastures grazed by sheep. Soil Biol Biochem 26:29–39, 1994.

Saggar, S., Andrew, R.M., Tate, K.R., Hedley, C.B., Rodda, N.J. and Townsend, J.A.: Modelling nitrous oxide emissions from dairy-grazed pastures. Nutr. Cycl. Agroecosyst 68**:**243–255, 2004

Saxton, K.E., Rawls, W.J., Romberger, J.S. and Papendick, R. I.: Estimating generalized soil-water characteristics from texture. Soil Sci. Soc. Amer. J. 50(4), 1031-1036, 1986.

Saxton, K.E. and Rawls, W.J.: Soil water characteristic estimates by texture and organic matter for hydrologic solutions. Soil Sci. Soc. Am. J. 70, 1569–1578, 2006.

Schmid, M., Neftel, A., Riedo, M. and Fuhrer, J.:. Process-based modelling of nitrous oxide emissions from different nitrogen sources in mown grassland. Nutr. Cycl. Agroecosyst. 60, 177-187, 2001.

Smith, K.A. and Massheder, J.: Predicting nitrous oxide emissions from N-fertilized grassland soils in the UK from three soil variables, using the B-LINE 2 model. Nutr Cycl Agroecosyst 98, 309–326, 2014.

van der Weerden, T.J., Clough, T.J. and Styles, T.M.: Using near-continuous measurements of N_2O emission from urine-affected soil to guide manual gas sampling regimes. New Zealand J. Agric. Res. 56, 60-76, 2013.

Yoshinari. T., Hynes, R. and Knowles, R.: Acetylene inhibition of nitrous oxide reduction and measurement of denitrification and nitrogen fixation in soil. Soil Biol. Biochem. 9, 177-183, 1977.

Table 1. Key soil properties of the Eutri-Stagnic Cambisol at Oensingen as used in *ecosys*.

Depth	**BD**[¶‡]	**TOC**	**TON**	**FC**[†]	**WP**[†]	**K_{sat}**[†]	**pH**	**Sand**[‡]	**Silt**[‡]	**Clay**[‡]	**CF**
m	Mg m^{-3}	g kg^{-1}	g kg^{-1}	m^3 m^{-3}	m^3 m^{-3}	mm h^{-1}		g kg^{-1}	g kg^{-1}	g kg^{-1}	m^3 m^{-3}
0.01	1.21	27.2	2.9	0.38	0.22	3.4	7	240	330	430	0
0.03	1.21	27.2	2.9	0.38	0.22	3.4	7	240	330	430	0
0.07	1.21	27.2	2.9	0.38	0.22	3.4	7	240	330	430	0
0.13	1.24	27.2	2.9	0.39	0.23	3.4	7	240	330	430	0
0.28	1.28	20.2	2.1	0.40	0.24	2.4	7	180	380	440	0
0.6	1.28	11.6	1.1	0.40	0.24	1.4	7	180	380	440	0
0.7	1.28	11.6	1.1	0.40	0.24	1.4	7	180	380	440	0
0.9	1.28	9	0.9	0.40	0.24	1.4	7	180	380	440	0
1.5	1.28	6	0.6	0.40	0.24	1.4	7	180	380	440	0.1

[¶] abbreviations BD: bulk density, TOC and TON: total organic C and N, FC: field capacity, WP: wilting point, K_{sat}: saturated hydraulic conductivity, CF: coarse fragments.

[‡] BD, TOC and texture were determined from soil cores taken in 2001 and 2006. Details are given in Leifeld et al. (2011).

[†] FC, WP and K_{sat} were estimated from BD, TOC and texture according to Saxton et al. (1996) and Saxton and Rawls (2006).

Table 2. Plant and soil management operations at the Oensingen intensively managed grassland from 2001 to 2009.

Year	Plant Management		Soil Management					
	Date	Management	Date	Management	Amount (g m^{-2})			
					NH_4^+	NO_3^-	ON	OC
2001			07 May	tillage				
			10 May	tillage				
	11 May	planting	15 June	mineral fertilizer	1.5	1.5		
	1 July	harvest	12 July	mineral fertilizer	1.5	1.5		
	8 Aug.	harvest	16 Aug.	mineral fertilizer	1.15	1.15		
	12 Sep.	harvest						
	31 Oct.	harvest						
2002			12 Mar.	mineral fertilizer	1.5	1.5		
	15 May	harvest	22 May	manure slurry	4.2		2.8	31.2
	25 June	harvest	1 July	mineral fertilizer	1.75	1.75		
	15 Aug.	harvest	18 Aug.	manure slurry	5.9		5.3	49.6
	18 Sep.	harvest	30 Sep.	mineral fertilizer	1.5	1.5		
	07 Dec.	harvest						
2003			18 Mar.	manure slurry	5.9		5.3	61.1
	30 May	harvest	02 June	mineral fertilizer	1.5	1.5		
	04 Aug.	harvest	18 Aug.	manure slurry	6.3		1.9	19.0
	13 Oct.	harvest						
2004			17 Mar.	manure slurry	5.0		1.5	19.5
	11 May	harvest	17 May	mineral fertilizer	1.5	1.5		
	25 June	harvest	01 July	manure slurry	5.5		0.5	9.9
	28 Aug.	harvest	31 Aug.	mineral fertilizer	1.5	1.5		
	03 Nov.	harvest						
2005			29 Mar.	manure slurry	6.7		3.1	42.0
	10 May	harvest	17 May	mineral fertilizer	1.5	1.5		
	27 June	harvest	05 July	manure slurry	5.0		3.5	59.6
	29 Aug.	harvest	16 Sep.	mineral fertilizer	1.5	1.5		
	24 Oct.	harvest						
2006	24 May	harvest						
	05 July	harvest	13 July	manure slurry	4.7		1.4	12.5
	12 Sep.	harvest	27 Sep.	manure slurry	4.4		1.3	13.6
	26 Oct.	harvest	30 Oct.	manure slurry	6.4		3.2	57.8

2007			03 Apr.	manure slurry	5.2		4.6	75.1
	26 Apr.	harvest	03 May	mineral fertilizer	1.5	1.5		
	06 July	harvest	13 July	manure slurry	4.9		1.8	45.9
	23 Aug.	harvest	28 Aug.	mineral fertilizer	1.5	1.5		
	11 Oct.	harvest	24 Oct.	manure slurry	4.6		3.0	38.9
	19 Dec.	terminate	19 Dec.	plowing				
2008			01 May	tillage				
			04 May	tillage				
	05 May	planting						
	01 July	harvest	10 July	mineral fertilizer	1.5	1.5		
	29 July	harvest	07 Aug.	mineral fertilizer	1.5	1.5		
	08 Sep.	harvest	19 Sep.	manure slurry	2.9		0.5	8.6
	07 Nov.	harvest						
2009			07 Apr.	mineral fertilizer	1.5	1.5		
	01 May	harvest	12 May	manure slurry	4.4		1.6	26.0
	16 June	harvest	06 Aug.	manure slurry	3.3		1.2	19.0
	29 July	harvest						
	07 Sep.	harvest	15 Sep.	mineral fertilizer	6.5(urea)			
	20 Oct.	harvest						

Table 3: Intercepts (*a*), slopes (*b*) coefficients of determination (R^2), ratios of mean squares for regression vs. error (F) and number of data pairs from regressions of (a) log-transformed 4-hour averages of N_2O fluxes (mg N m^{-2} h^{-1}) modelled vs. measured during each year from 2004 to 2009, and (b) total N_2O fluxes (mg N m^{-2}) modelled vs. measured during emission events following each fertilizer or manure application from 2004 to 2009 (see Fig. 3) at the Oensingen intensively managed grassland.

Year	***a***	***b***	**R^2**	**F‡**	***n***
(a)					
2004	$1.25 \pm 0.88 \times 10^{-5}$	0.49 ± 0.06	0.08	69	818
2005	$1.63 \pm 0.43 \times 10^{-5}$	0.59 ± 0.03	0.24	368	1173
2006	$4.28 \pm 0.44 \times 10^{-5}$	1.04 ± 0.08	0.14	155	948
2007	$1.21 \pm 0.33 \times 10^{-5}$	0.67 ± 0.02	0.35	989	1794
2008	$1.44 \pm 0.51 \times 10^{-5}$	0.44 ± 0.03	0.08	157	1703
2009	$-0.03 \pm 0.25 \times 10^{-5}$	0.71 ± 0.02	0.49	1574	1614
(b)					
2004 - 2009	28 ± 9 mg N m^{-2}	0.67 ± 0.13	0.54	27	23

‡ All values of F were highly significant ($P < 0.001$).

Table 4. Annual gross primary productivity (GPP), ecosystem respiration (R_e), net ecosystem productivity (NEP = GPP - R_e), harvest, net biome productivity (NBP) and N_2O emissions derived from EC or chambers and modelled (M) with current land management (Table 2), and with defoliation increased so that LAI remaining after harvesting was reduced by one-half (1/2), with defoliation increased and delayed by 5 days (1/2 + 5d),. Positive values indicate uptake, negative values emissions.

Year		2002	2003	2004	2005	2006	2007	2008	2009
Precip.(mm)		1478	817	1158	966	1566	1328	1188	1004
MAT (^oC)		9.56	9.58	8.92	8.67	9.30	9.59	9.30	9.48
GPP	EC	2159	1773	2058	1766	1817	2102	1455	2119
(g C m^{-2} y^{-1})	M: current	2214	1836	2220	2111	1953	2539	1419	1852
	: 1/2	2064	1764	2054	1969	1865	2285	1305	1705
	: 1/2 + 5d	2014	1774	2076	1966	1771	2277	1225	1686
R_e	EC	-1490	-1558	-1541	-1565	-1577	-1684	-1450	-1657
(g C m^{-2} y^{-1})	M: current	-1560	-1421	-1704	-1679	-1680	-1935	-1366	-1373
	: 1/2	-1457	-1345	-1569	-1572	-1579	-1714	-1212	-1259
	: 1/2 + 5d	-1458	-1350	-1541	-1517	-1519	-1679	-1183	-1235
NEP	EC	669	215	517	201	240	418	5	462
(g C m^{-2} y^{-1})	M: current	654	415	516	432	273	604	53	479
	: 1/2	607	419	485	397	286	571	93	446
	: 1/2 + 5d	556	414	535	449	252	598	42	451
Harvest	field	462	241	401	247	232	448	293	532
(g C m^{-2} y^{-1})	M: current	570	314	525	460	421	690	308	487
	: 1/2	561	360	465	497	455	678	314	484
	: 1/2 + 5d	537	353	579	513	446	686	262	473
C inputs		81	80	29	102	84	160	9	45
NBP	field	288	54	145	56	92	130	-279	-25
(g C m^{-2} y^{-1})	M: current	165	181	20	74	-64	74	-246	37
	: 1/2	127	139	49	2	-85	53	-212	7
	: 1/2 + 5d	101	141	-15	38	-110	72	-211	23
N inputs		27.6	22.5	18.5	24.3	21.4	30.1	9.4	20.0
N_2O	chamber								
(g N m^{-2} y^{-1})	upper bound	-0.130	-0.050	-0.060	-0.230	-0.020	-0.280	-0.480	-0.510
	lower bound	-0.450	-0.180	-0.180	-0.320	-0.060	-0.350	-0.620	-0.680
	M: current	-0.302	-0.209	-0.183	-0.193	-0.220	-0.281	-0.326	-0.366
	: 1/2	-0.269	-0.215	-0.250	-0.249	-0.318	-0.312	-0.335	-0.318
	: 1/2 + 5d	-0.284	-0.234	-0.347	-0.352	-0.273	-0.348	-0.327	-0.395

Table 5. Annual N_2O emissions modelled with current field management (Table 2) and soil properties (Table 1) (current), with soil bulk density (BD) increased by 5% and 10% to a depth of 3 cm, and with the Michaelis-Menten constants for reduction of O_2 (K_{O_2}) and of NO_3^- and NO_2^- (K_{NO_x}) halved or doubled from those used in the model.

Year		2002	2003	2004	2005	2006	2007	2008	2009
Precip.(mm)		1478	817	1158	966	1566	1328	1188	1004
MAT (^{o}C)		9.56	9.58	8.92	8.67	9.30	9.59	9.30	9.48
N_2O (g N m^{-2} y^{-1})	current	-0.302	-0.209	-0.183	-0.193	-0.220	-0.281	-0.326	-0.366
	BD + 5%	-0.352	-0.213	-0.218	-0.199	-0.309	-0.332	-0.358	-0.372
	BD + 10%	-0.334	-0.235	-0.231	-0.236	-0.336	-0.374	-0.424	-0.371
	K_{O2} x 0.5	-0.250	-0.179	-0.154	-0.159	-0.160	-0.216	-0.276	-0.349
	K_{O2} x 2.0	-0.390	-0.263	-0.221	-0.247	-0.315	-0.385	-0.381	-0.468
	K_{NOx} x 0.5	-0.382	-0.261	-0.265	-0.267	-0.262	-0.378	-0.432	-0.457
	K_{NOx} x 2.0	-0.234	-0.163	-0.126	-0.132	-0.126	-0.208	-0.232	-0.288

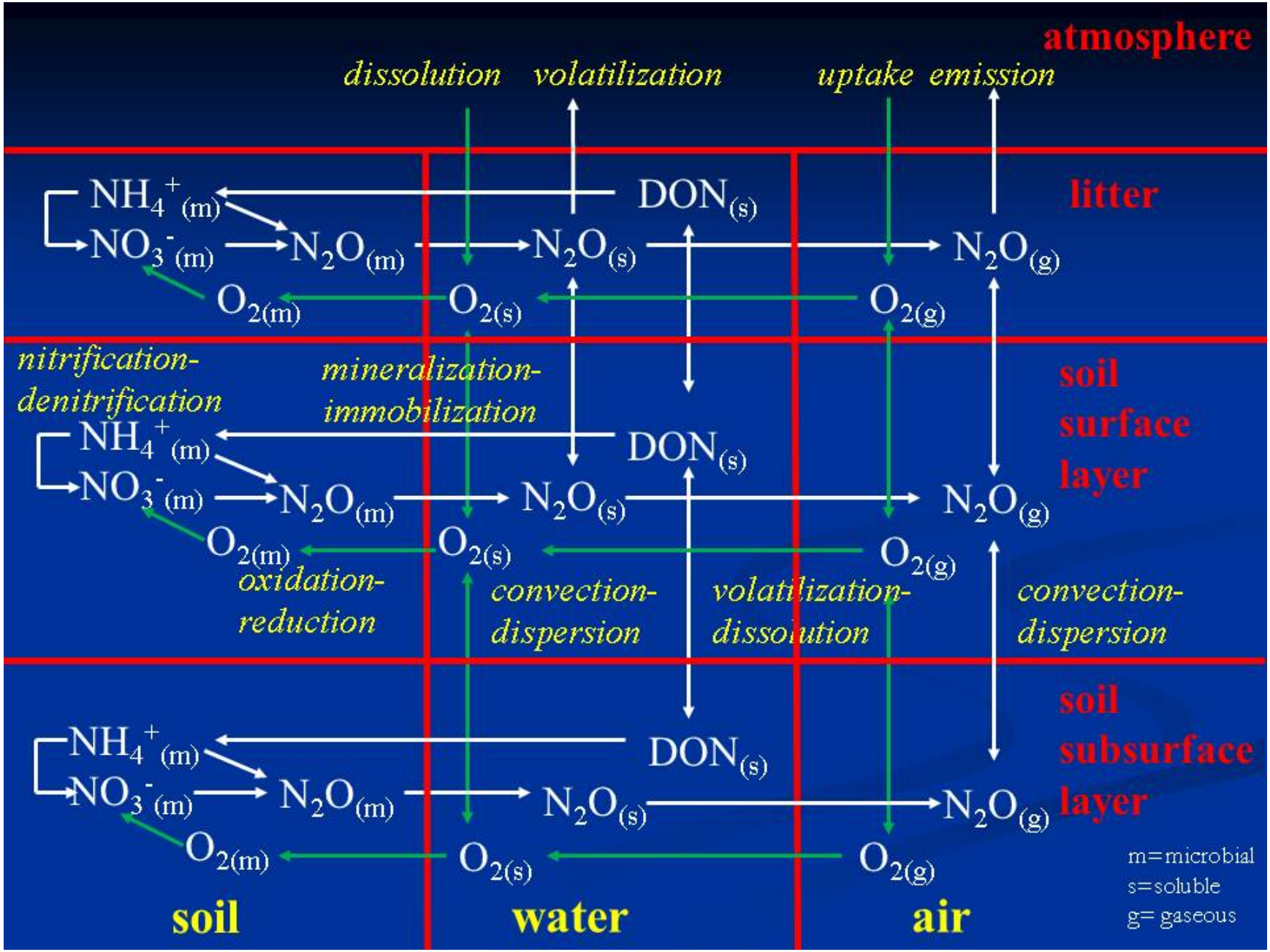

Fig. 1: Summary of key processes governing generation and emission of N_2O as represented in *ecosys*.

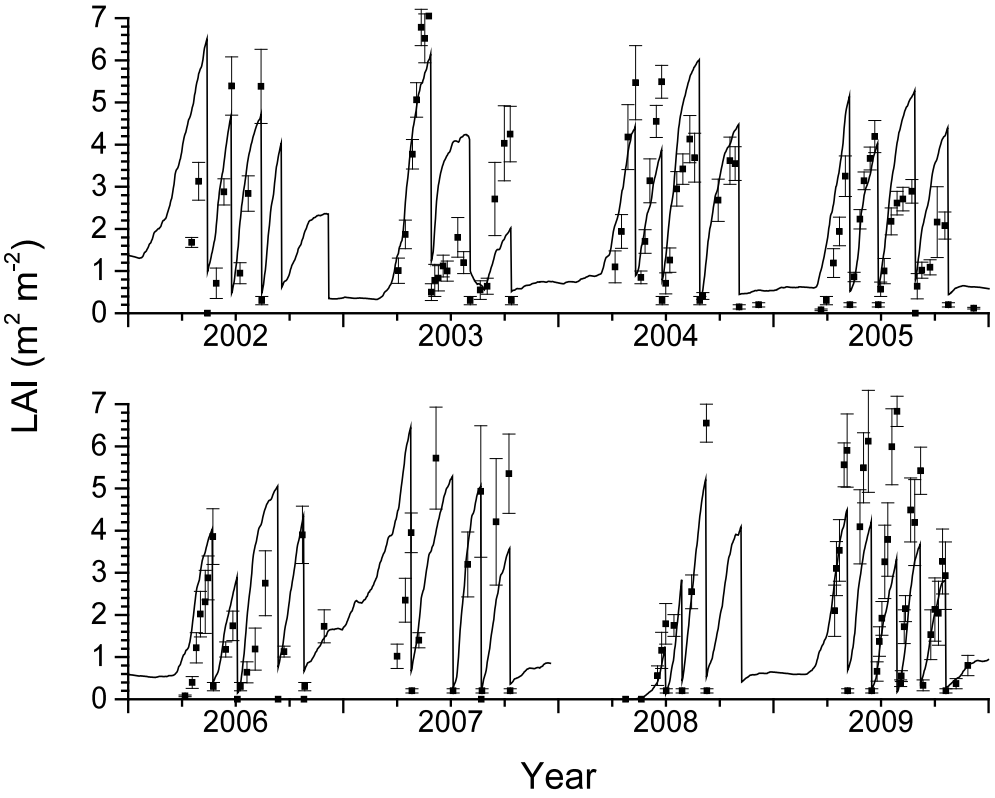

Fig. 2. LAI measured (symbols) and modelled (lines) from 2002 through 2009 at the Oensingen intensively managed grassland.

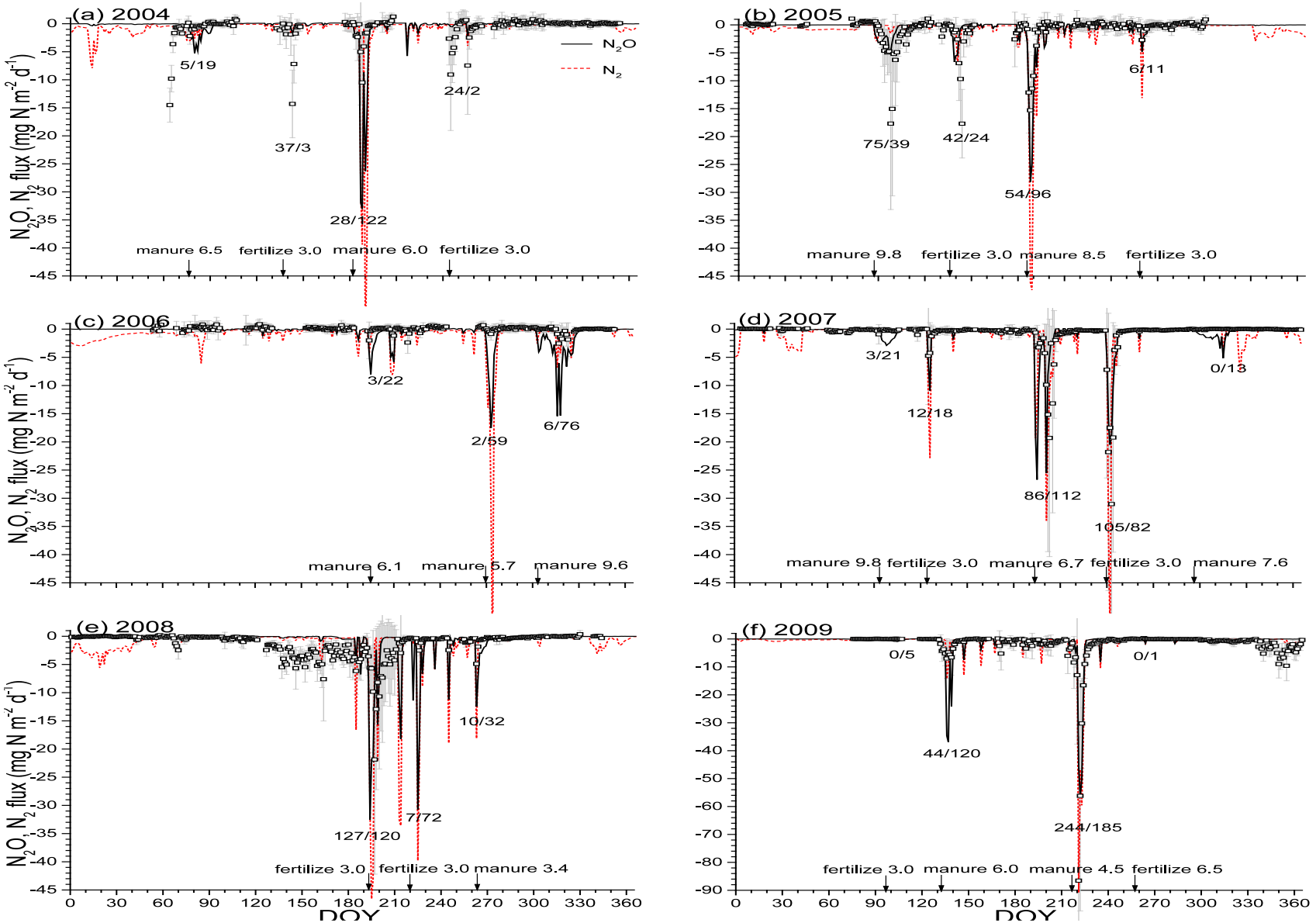

Fig. 3. Daily-aggregated N_2O emissions measured (symbols) and N_2O and N_2 emissions modelled (lines) from 2004 through 2009 at the Oensingen intensively managed grassland. Numbers above and beside each fertilizer or manure addition indicate total measured/modelled N_2O-N emitted during emission events (mg N m^{-2}), and total N applied (g N m^{-2}). Negative values indicate effluxes to the atmosphere.

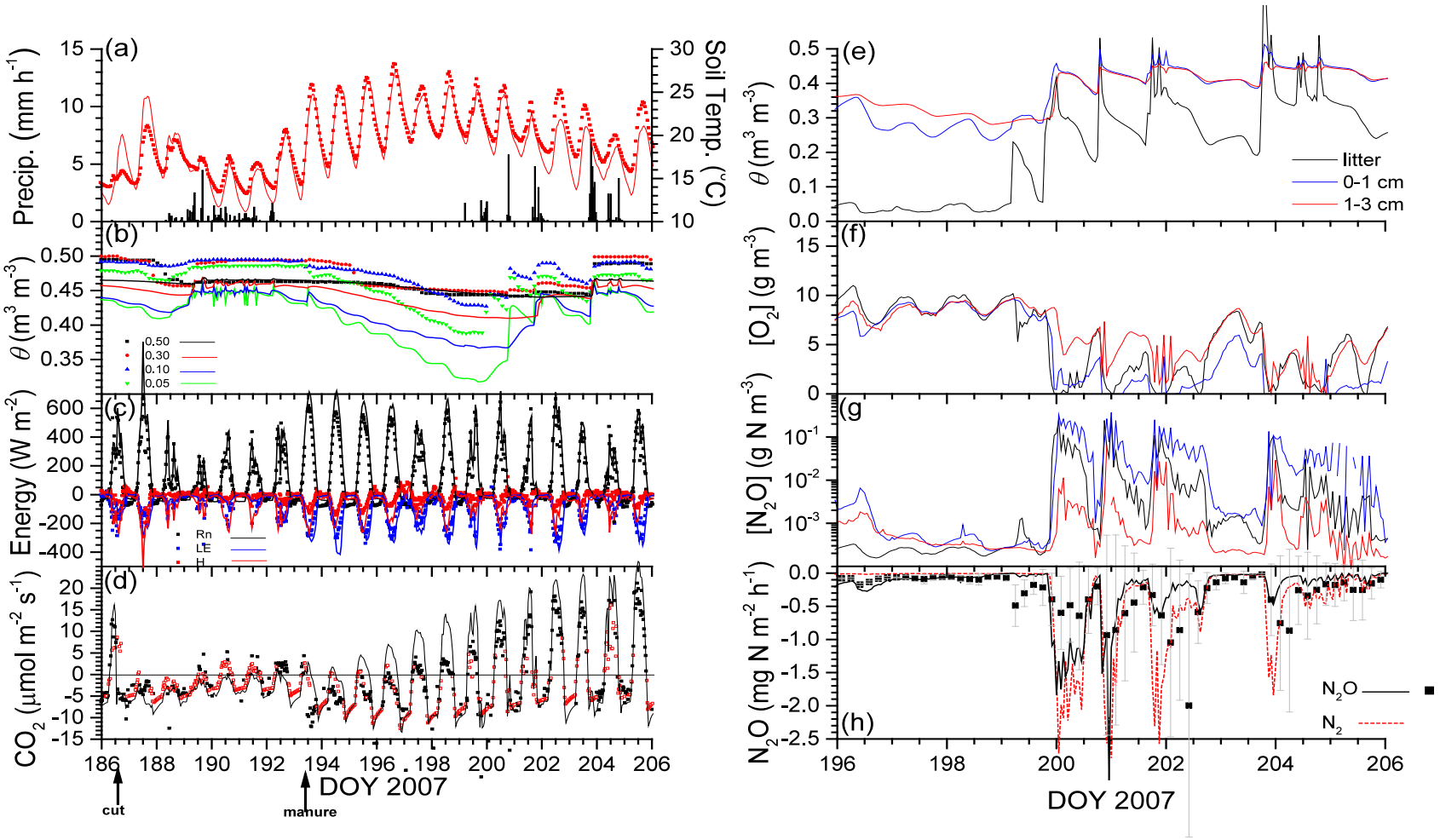

Fig. 4. (a) Precipitation and soil temperature at 0.05 m, (b) soil water content (θ) at 0.05, 0.10, 0.30 and 0.50 m, (c) energy and (d) CO_2 fluxes measured (closed symbols), gap-filled (open symbols) and modelled (lines) during 20 days from harvest (cut) to the end of the emission event following manure application (manure) in July 2007. (e) θ, (f and g) aqueous concentrations of O_2 and N_2O modelled in the surface litter and at 0.01 and 0.02 m in the soil, and (h) N_2O and N_2 fluxes measured (symbols) and modelled (lines) during the last 10 days of this period when the emission event occurred. For fluxes, positive values represent influxes to the soil, negative values effluxes to the atmosphere.

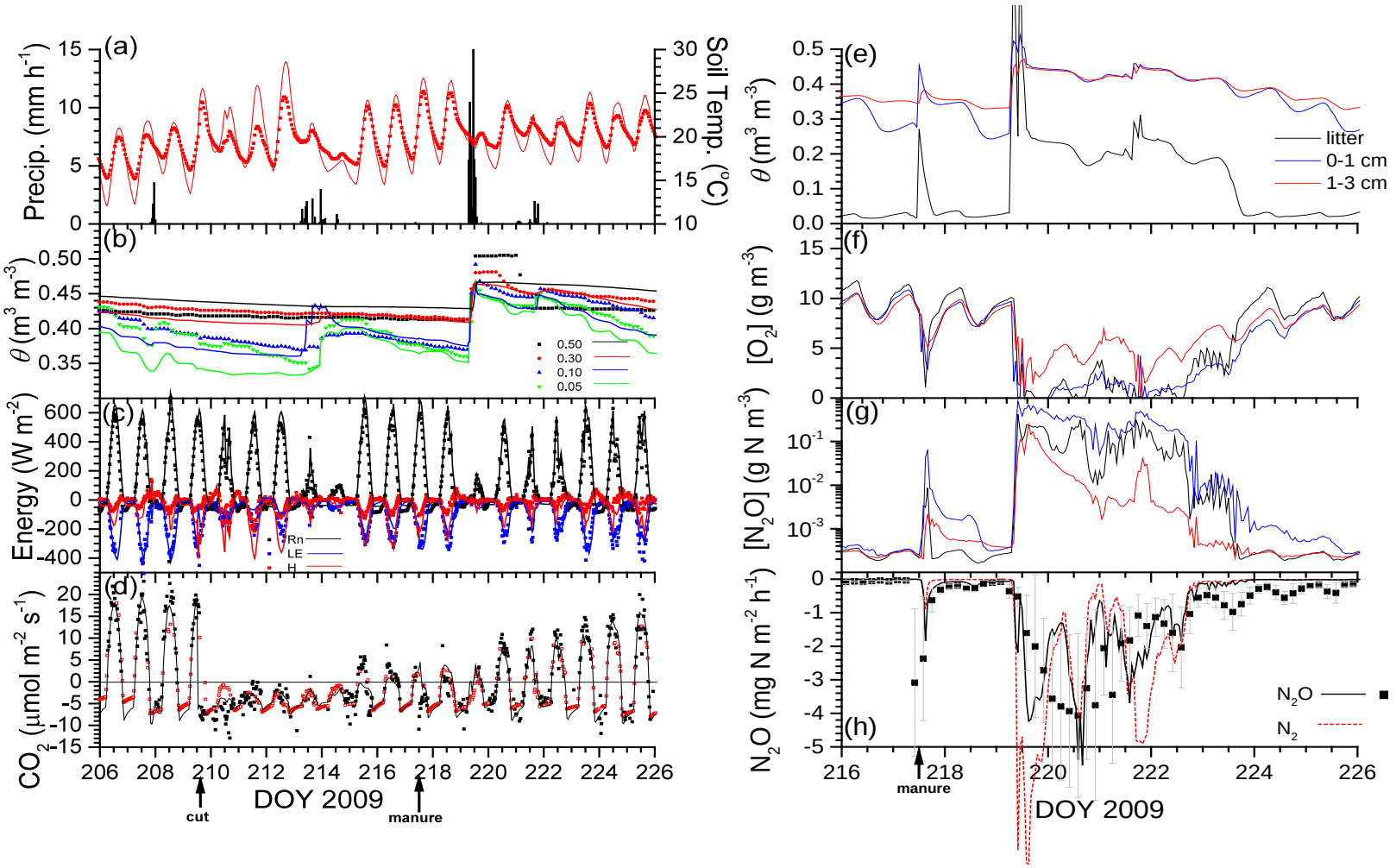

Fig. 5. (a) Precipitation and soil temperature at 0.05 m, (b) soil water content (θ) at 0.05, 0.10, 0.30 and 0.50 m, (c) energy and (d) CO_2 fluxes measured (closed symbols), gap-filled (open symbols) and modelled (lines) during 20 days from harvest (cut) to the end of the emission event following manure application (manure) in August 2008. (e) θ, (f and g) aqueous concentrations of O_2 and N_2O modelled in the surface litter and at 0.01 and 0.02 m in the soil, and (h) N_2O and N_2 fluxes measured (symbols) and modelled (lines) during the last 10 days of this period when the emission event occurred. Positive flux values represent influxes to the soil, negative values effluxes to the atmosphere.

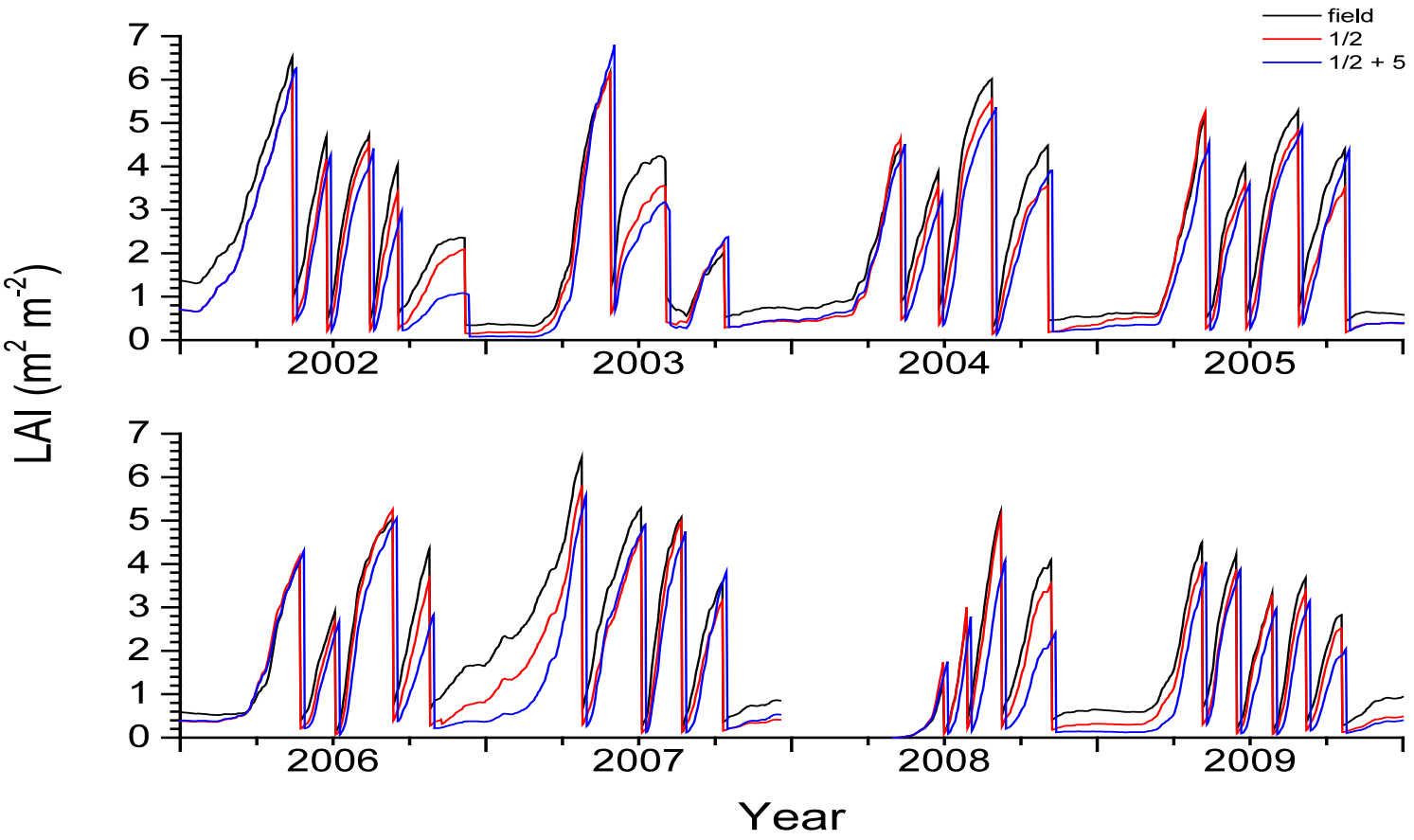

Fig. 6. LAI modelled from 2002 through 2009, with LAI after each cut reduced to one-half of that estimated from the field experiment without or with a delay of 5 days at the Oensingen intensively managed grassland.

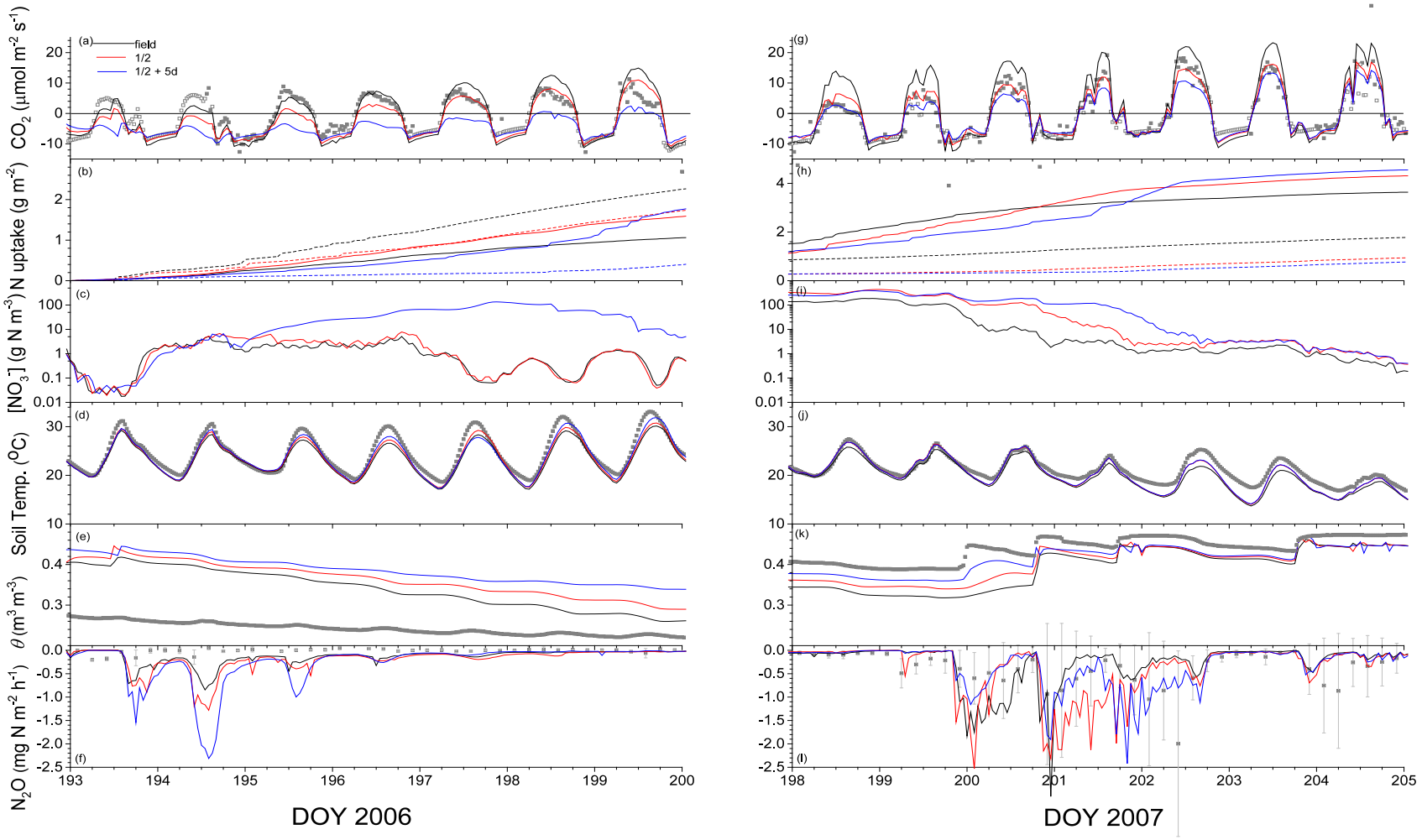

Fig. 7. (a,g) CO_2 fluxes, (b,h) cumulative NH_4^+ (dashed) and NO_3^- (solid) uptake since manure application, (c,i) aqueous NO_3^- concentrations at 0 – 1 cm, (d,j) T_s and (e,k) θ at 5 cm, and (f,l) N_2O fluxes measured (symbols) and modelled (lines) with LAI after each cut reduced to one-half of that estimated from the field experiment without or with a delay of 5 days during emission events following manure applications on DOY 194 in (a-f) 2006 and (g-l) 2007 (see Table 2). For fluxes, positive values represent influxes to the soil, negative values effluxes to the atmosphere.

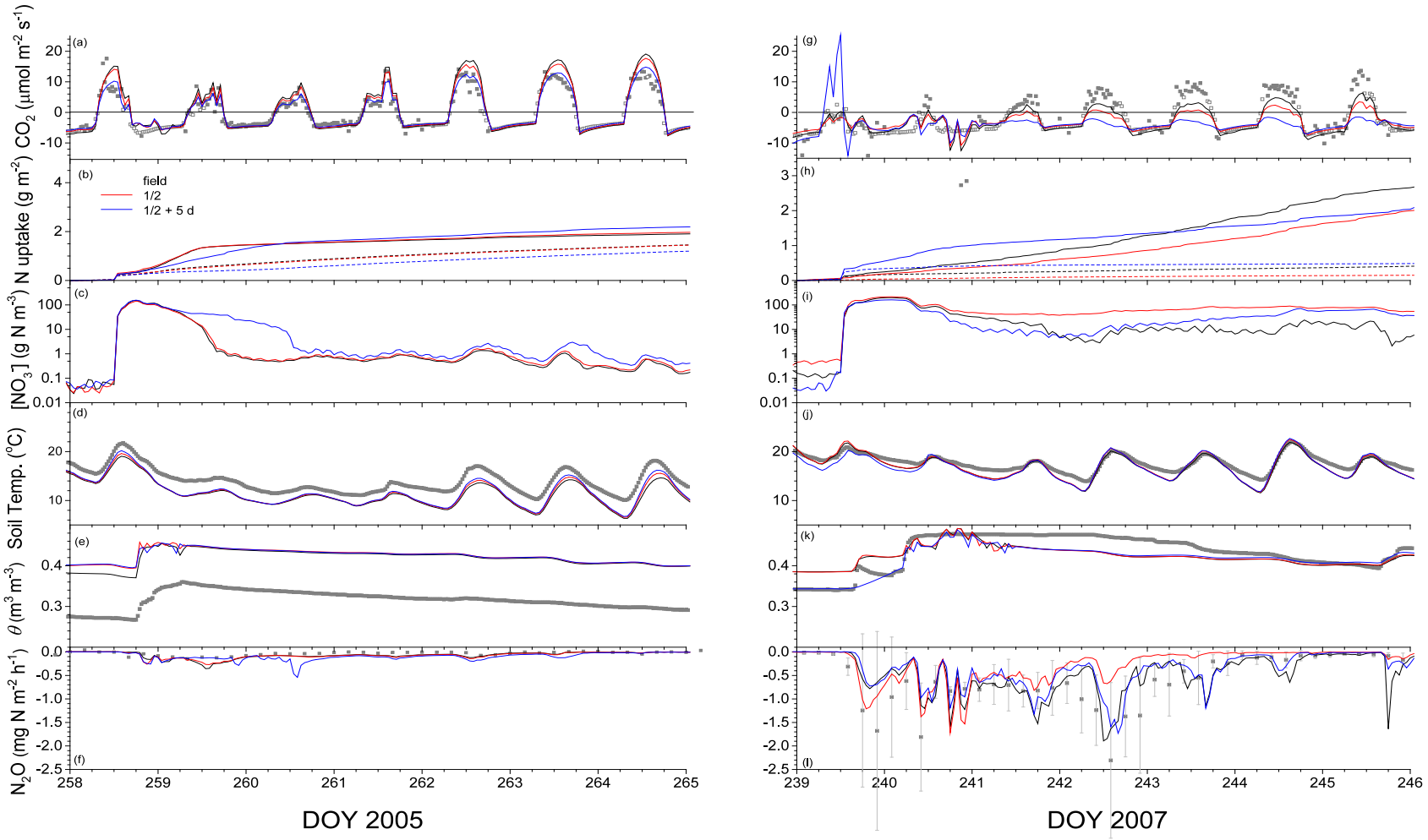

Fig. 8 (a,g) CO_2 fluxes, (b,h) cumulative NH_4^+ (dashed) and NO_3^- (solid) uptake since fertilizer application, (c,i) aqueous NO_3^- concentrations at 0 – 1 cm, (d,j) T_s and (e,k) θ at 5 cm, and (f,l) N_2O fluxes measured (symbols) and modelled (lines) with LAI after each cut reduced to one-half of that estimated from the field experiment without or with a delay of 5 days during emission events following fertilizer applications on DOY 259 in 2005 (a-f) and DOY 240 in 2007 (g-l) (see Table 2). For fluxes, positive values represent influxes to the soil, negative values effluxes to the atmosphere.

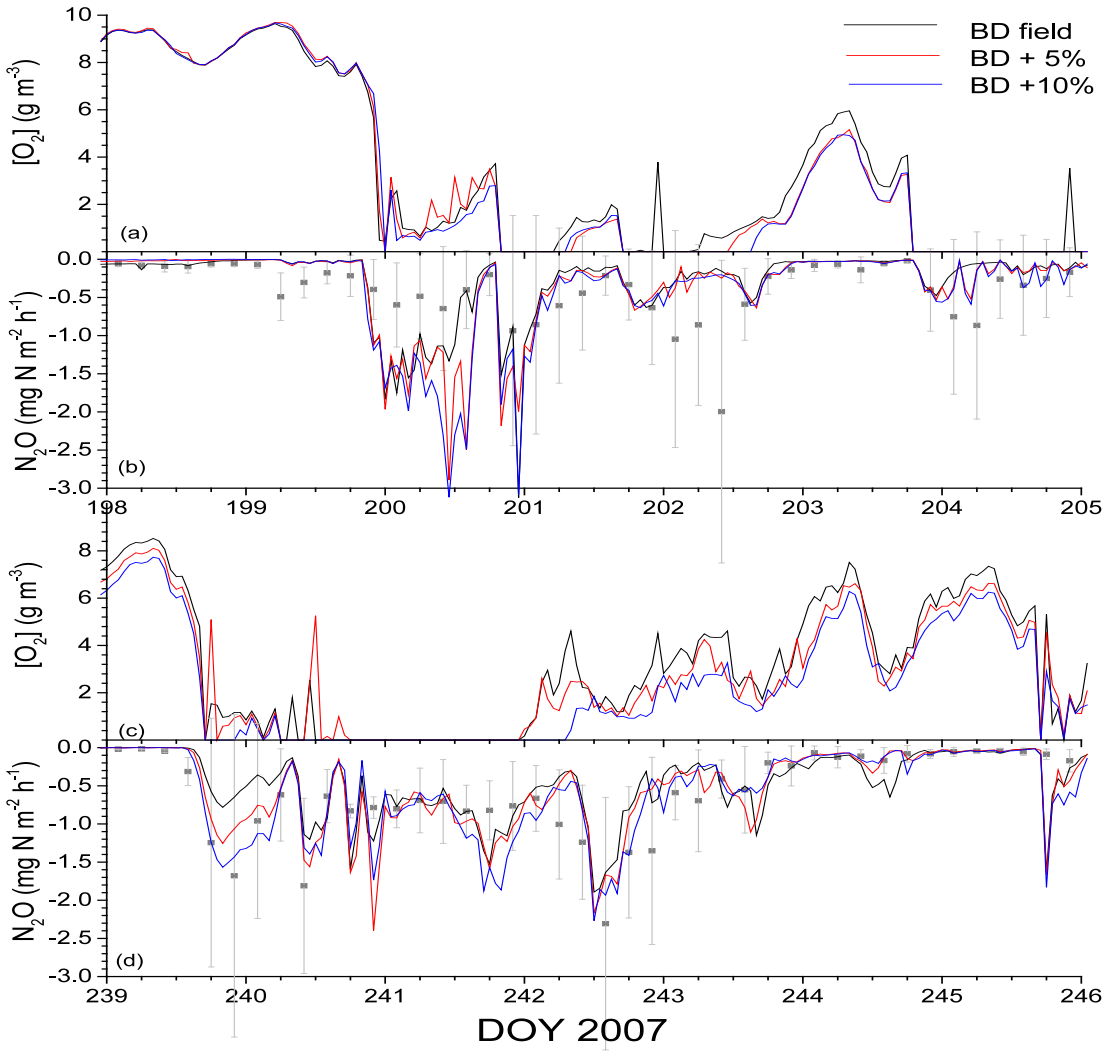

Fig. 9. (a,c) Aqueous O_2 concentrations, and (b,d) N_2O fluxes measured (symbols) and modelled (lines) with bulk density (BD) from field measurements, and with BD raised by 5% or 10% following (a,b) manure application on DOY 194 and (c,d) fertilizer application on DOY 240 in 2007 (see Table 2). For fluxes, positive values represent influxes to the soil, negative values effluxes to the atmosphere.